https://doi.org/10.5194/egusphere-2025-3151
Preprint. Discussion started: 30 July 2025

Air quality impacts of Stratospheric Aerosol Injections are small and mainly driven by changes in climate, not deposition

Cindy Wang[1], Daniele Visioni[1], Glen Chua[2], and Ewa M. Bednarz[3,4]

[1]Department of Earth and Atmospheric Sciences, Cornell University, Ithaca, NY, USA
[2]NASA Goddard Institute for Space Studies, NY, NY, USA
[3]Cooperative Institute for Research in Environmental Sciences (CIRES), University of Colorado Boulder, Boulder, CO, USA
[4]NOAA Chemical Sciences Laboratory (NOAA CSL), Boulder, CO, USA

Correspondence: Cindy Wang (cindywang@cornell.edu)

Abstract. Stratospheric aerosol injection (SAI) is a proposed climate intervention that could potentially reduce future global warming, but its broader environmental and public health implications are yet to be thoroughly explored. Here, we assess changes in mortality attributable to fine particulate matter ($PM_{2.5}$) and ozone (O_3) using three large ensembles of fully coupled CESM2-WACCM6 simulations from the ARISE-SAI-1.5, ARISE-SAI-1.0 and SSP2-4.5 scenarios. In the ARISE-SAI-1.5 scenario, maintaining temperatures at 1.5 degrees above preindustrial levels through SAI results in a modest reduction in pollution-related mortality during 2060–2069 relative to SSP2-4.5, driven by a 1.26% decrease in ozone-related deaths and a 0.86% increase in $PM_{2.5}$-related deaths. $PM_{2.5}$ mortality changes exhibit almost no sensitivity to injected sulfate amounts, with the most variability driven by precipitation-mediated changes in non-sulfate $PM_{2.5}$ species (e.g., dust and secondary organic aerosols), whereas ozone-related mortality are primarily driven by surface cooling and hemispheric asymmetries in stratospheric-tropospheric exchange and ozone transport. Overall, SAI impacts on pollution-related mortality are modest, regionally heterogeneous, and much smaller in magnitude compared to improvements expected from near-term air quality policies. Our finding that mortality impacts do not directly scale with SO_2 injection rates underscores the nonlinear and complex nature of atmospheric responses to SAI. Significant differences across ensemble members further emphasize the role of internal variability and the need for ensemble-based analysis when evaluating potential health implications of climate intervention strategies.

1 Introduction

Stratospheric aerosol injection (SAI) is a proposed climate intervention strategy to ameliorate global warming. It involves releasing reflective aerosols–usually sulfates–into the stratosphere to increase Earth's albedo and lower temperatures. This approach draws on the observed cooling effects of large volcanic eruptions (McCormick et al., 1995; Robock, 2000) and has been shown in climate model simulations to reduce global mean surface temperatures relatively effectively (Tilmes et al., 2018; Kravitz et al., 2015). However, despite its potential to offset some of the warming caused by greenhouse gases, SAI raises numerous questions regarding its broader environmental, societal, and health-related consequences. One key concern is the impact of SAI on public health and air quality (Tracy et al., 2022). In terms of air quality, the main drivers of changes

https://doi.org/10.5194/egusphere-2025-3151
Preprint. Discussion started: 30 July 2025

would include the direct impacts of sulfate particles on surface fine particulate matter ($PM_{2.5}$), and changes in surface ozone (O_3); the latter would be a function of changes in stratosphere-to-troposphere O_3 transport and in-situ changes in tropospheric ozone chemistry driven by the SAI-induced changes in temperatures and photolysis.

This study aims to assess the effects of SAI on air pollution mortality, particularly through changes in surface $PM_{2.5}$ and surface ozone (O_3), by using a fully-coupled modeling approach with the Community Earth System Model (CESM2) Whole Atmosphere Climate-Chemistry Model (WACCM6) with comprehensive stratospheric and tropospheric chemistry. While using non-coupled model approaches allow one to better separate and quantify the contribution of single factors, a fully-coupled model allows for the simulation to include their interaction: what might be lost in precision in the diagnosis of changes can be gained in providing a more holistic picture of the overall expected change.

Previous studies have looked into the health impacts of SAI due to air quality changes (Eastham et al., 2018; Visioni et al., 2020; Moch et al., 2023; Harding et al., 2024). These efforts have either relied on more idealized modeling frameworks and/or simplified mortality estimation methods. In particular, both Eastham et al. (2018) and Moch et al. (2023) used chemical transport models (CTMs) to quantify global mortality effects from SAI, including contributes from changes in air quality and UV-B exposure. While CTMs like GEOS-Chem have been widely applied to study air-pollution-related health outcomes (Norman et al., 2025), they are fundamentally limited in capturing the dynamical and chemical feedbacks relevant to SAI. For example, in Eastham et al. (2018), the aerosol size distribution was prescribed offline assuming a fixed lognormal distribution centered at 0.16 μm. The use of a CTM also precludes accounting for interactive changes in stratosphere–troposphere exchange (STE), temperature-dependent tropospheric chemistry, and large-scale circulation responses to SAI. As a result, such models tend to predict spatially uniform decreases in stratospheric ozone and, consequently, reductions in tropospheric ozone via STE, without accounting for compensating changes in transport or chemistry.

Harding et al. (2024) further used similar estimates as Eastham et al. (2018) and compared them against estimates of SAI impact on temperature-attributable mortality in the GFDL/FLOR model, in which the radiative forcing from geoengineering was simulated by reducing the solar constant. While solar dimming provide a simplified means of approximating the cooling effects of geoengineering, they do not account for the spectrally dependent scattering and absorption properties of stratospheric aerosols, nor do they adequately capture the associated chemical and dynamical feedbacks, particularly those influencing ozone and STE (Visioni et al., 2021; Bednarz et al., 2022).

Finally, Xia et al. (2017) examined the impacts of SAI on tropospheric ozone through the use of a low-top version of CESM2, simulating SAI itself through prescribing an aerosol distribution (therefore with no changes in stratospheric aerosols settling and deposition) or through a solar constant reduction; they found that surface ozone generally decreases as a consequence of SAI, with some significant differences between solar dimming and SAI driven by changes in stratospheric ozone and STE, but did not quantify the the resulting health implications of changes in surface ozone.

In this study, we use simulations from the Assessing Responses and Impacts of Solar intervention on the Earth system with Stratospheric Aerosol Injection experiment using CESM2-WACCM6, which simulates SAI with injections at four discrete latitudinal points (15°S, 15°N, 30°S and 30°N) in order to maintain large scale surface temperatures at the 1.5°C (ARISE-SAI-1.5) or 1.0°C (ARISE-SAI-1.0) above preindustrial levels (Davis et al., 2023). This model includes comprehensive atmospheric

https://doi.org/10.5194/egusphere-2025-3151
Preprint. Discussion started: 30 July 2025

chemistry and interactive aerosol processes, allowing for a more detailed assessment of how SAI influences air pollution and associated health risks, as well as interactively simulating the coupling between SAI-induced changes in atmospheric temperatures, transport and chemistry. Compared to previous studies, our approach provides a more realistic representation of injection strategies and chemistry-climate interactions, improving estimates of pollution-driven mortality. Another key contribution of this study is the explicit quantification of model internal variability in estimates of air pollution and associated health impacts. Modeled air pollutant concentrations are sensitive to changes in climate and dynamics which in turn are affected by model internal variability. This could be especially important when the changes in surface air pollution arise from climate system adjustments due to SAI rather than from changes in surface emissions. While this source of uncertainty is often underexplored in the literature (e.g. it cannot be easily assessed based on CTM results), our use of a 10-member ensemble of coupled simulations allows us to highlight its substantial influence on $PM_{2.5}$ annd ozone concentrations, and the associated mortality outcomes. In the following sections, we evaluate the effects of SAI on surface air quality and associated health outcomes by analyzing changes in $PM_{2.5}$ and ozone exposure, estimating attributable mortality using epidemiological risk functions, and characterizing the spatial and ensemble variability in these impacts on global and regional scales.

2 Methods

2.1 Simulations

Simulations were conducted using the Community Earth System Model, version 2 with the WACCM, version 6 (CESM2(WACCM6); Gettelman et al. (2019); Davis et al. (2023)), a fully coupled ocean-atmosphere model with interactive tropospheric and stratospheric chemistry and aerosols. The model simulates aerosol formation and growth through an interactive, two-moment modal aerosol microphysics scheme (MAM4; Liu et al. (2016)), allowing sulfate aerosols to evolve over time based on the simulation of nucleation, coagulation, condensation and removal processes. However, it is to be noted that MAM4 uses assumptions of internal mixing for the size distribution of different species (whereas mass is tracked separately) (Visioni et al., 2022). While stratospheric and tropospheric chemistry are fully interactive, tropospheric photolysis rates are prescribed and held constant at year-2000 levels (Kinnison et al., 2007). Sulfate (SO_4), secondary organic aerosols (SOA), primary organic matter (POM), salt, dust and black carbon (BC) are simulated and considered for calculating $PM_{2.5}$.

The SSP2-4.5 ensemble represents a control climate scenario following the Shared Socioeconomic Pathway 2 with moderate greenhouse gas emissions, leading to a radiative forcing of 4.5 W/m^2 by 2100 Fricko et al. (2017). The ARISE-SAI-1.5 experiment (Richter et al., 2022) simulates the deployment of stratospheric aerosol injection (SAI) to limit global warming to approximately 1.5°C above preindustrial levels (Richter et al., 2022). In ARISE-SAI-1.5, sulfur dioxide (SO_2) is injected annually at four fixed latitudes (15°N, 15°S, 30°N, 30°S) at approximately 21.5 km of altitude starting in year 2035 of SSP2-4.5, and run until 2070, with injection rates adjusted at the beginning of each year to offset continuing warming under the SSP2-4.5 emissions pathway and maintain global mean surface temperatures and their large-scale gradients at the 1.5C above preindustrial levels (defined as the mean over 2020-2039). The ARISE-SAI-1.0 simulations follow the same protocol, but cool by a further 0.5°C compared to ARISE-SAI-1.5.

https://doi.org/10.5194/egusphere-2025-3151
Preprint. Discussion started: 30 July 2025

A 10-member ensemble is used for all three ensembles to account for internal climatic variability (Richter et al., 2022). For regional assessments of mortality and mortality-related factors, we will focus our analyses on the ARISE-SAI-1.5 case, whereas results from the ARISE-SAI-1.0 will be provided for global, temporal and injection-related analyses in order to highlight the linearity (or lack thereof) of the response with the injection rates.

2.2 Calculation of exposure and mortality

We calculate the impact on mortality rates attributed to changes in ambient surface $PM_{2.5}$ and O_3 calculations. All mortality estimates in future scenarios are calculated using the fixed 2020 population distribution. This approach isolates the effects of air quality changes by removing confounding influences from projected population growth or redistribution. Mortality is estimated as follows:

$$M_{i,d,a,t} = \text{BMR}_{d,a,t} \times \text{P}_{i,a,2020} \times AF_{i,d,a,t} \tag{1}$$

Where $M_{i,t}$ is the mortality for CESM grid i from disease d for age group a and year t; P is the number of population in 2020 with each age group a in grid i; BMR is the national base mortality rate for disease d, age group a and year t; AF is the attributable fraction which estimates the proportion of deaths in a population that can be attributed to a specific exposure to disease d or risk factor from epidemiological studies. For $PM_{2.5}$, we use the AF associated with noncommunicable diseases and lower respiratory infections (NCD+LRI). For ozone, we use the AF associated with cardiovascular and respiratory diseases. Whereas previous studies (Eastham et al., 2018) attributed $PM_{2.5}$ exposure to cardiovascular and respiratory diseases and ozone exposure solely to respiratory diseases, we attribute cardiovascular disease to ozone exposure in this study which aligns with more recent epidemiological findings (Sun et al., 2024; Niu et al., 2022) and improves the completeness of ozone-related health impact assessments.

For $PM_{2.5}$, AF is calculated using the exposure–response function from the Global Exposure Mortality Model (GEMM), which provides improved estimates across a wide range of ambient $PM_{2.5}$ concentrations. GEMM is particularly effective in low-income and high-pollution regions where the older Integrated Exposure–Response (IER) functions tend to underperform due to limited observational data and less robust extrapolation at high exposure levels (Burnett et al., 2014, 2018; Burnett and Cohen, 2020):

$$AF_{i,d,a,t} = 1 - \frac{1}{RR_{i,d,a,t}}; \text{ where } RR_{i,d,a,t} = \exp^{\frac{\theta \times log(\frac{\text{C}_{i,t}}{\alpha+1})}{1+\exp^{-\frac{\text{C}_{i,t}-\mu}{v}}}} \text{ and } RR_{i,d,a,t} = 1 \text{ when } \text{C}_{i,t} < 2.4 \tag{2}$$

Where C is the ambient $PM_{2.5}$ concentration; θ, α, μ and v are parameters specified for each age group.

For ozone-attributable mortality, we convert surface ozone to the ozone season maximum daily 8-hour average (OSMDA8) using hourly surface O_3 data for each experiment and each ensemble member. OSMDA8 calculates the highest daily 8-hour average ozone concentration during the ozone season, which typically spans from spring through summer when ozone levels are at their peak. OSMDA8 is the metric used by the Global Burden of Disease (GBD) (Brauer et al., 2024) for quantifying the

https://doi.org/10.5194/egusphere-2025-3151
Preprint. Discussion started: 30 July 2025

health effect from long-term ozone exposure and is used in the World Heath Organization's air quality guidelines (Organization et al., 2021). To calculate the ozone-attributable risk fraction, we calculate the AF for cardiovascular and respiratory disease separately and then combine the associated mortality.

$$AF_{i,d,a,t} = 1 - \exp^{-\beta(\mathrm{X}_{i,t} - \mathrm{X}_{\mathrm{min}})}\text{; where } AF = 0 \text{ when } \mathrm{X}_{i,t} < \mathrm{X}_{\mathrm{min}} \tag{3}$$

Where X represents the spatially and temporally resolved grid-cell level OSMDA8; $\mathrm{X}_{\mathrm{min}}$ represents the theoretical minimum risk exposure concentration and β represents a model-parameterized slope of the log-linear relationship between concentration and health from epidemiological studies. For chronic respiratory disease mortality, we apply a β of $\ln(1.06)$ per 10 ppb ozone (95% CI 1.03-1.10) derived by GBD 2019 (Jerrett et al., 2009; Malashock et al., 2022; Murray et al., 2020). For cardiovascular disease mortality, we apply a β of $\ln(1.028)$ per 10 ppb ozone (95% CI 1.010-1.047) (Sun et al., 2024). A summary of the RR and disease d used to calculate mortality associated with $PM_{2.5}$ and O_3 is provided in Table 1.

Cause	Disease (d)	Minimum exposure concentration	Source
$PM_{2.5}$	Noncommunicable diseases & lower respiratory infections (NCD+LRI)	2.5 ppm	Burnett et al. (2018)
Ozone	Cardiovascular diseases	40 ppb	Sun et al. (2024)
	Respiratory diseases	32.4 ppb	Malashock et al. (2022)

Table 1. Summary of risk functions used for estimating attributable mortality. Minimum exposure concentrations correspond to the theoretical minimum risk exposure levels for each pollutant-health outcome pair.

Our baseline mortality rates (BMRs) are drawn from the International Futures (IFs) health model, providing dynamic, age and disease-specific mortality projections consistent with policy interventions following the SSP2-4.5 scenario (Hughes et al., 2014). The IFs health model, developed at the University of Denver's Pardee Center, is a comprehensive, integrated modeling platform used to explore long-term global health dynamics. This represents a more realistic approach compared to the use of static BMRs in previous studies (Eastham et al., 2018).

Population (P) for each age group was calculated by using the global population density dataset based on Shared Socioeconomic Pathways (SSP) (Jones and O'Neill, 2020) and the ratio of the population for each age group to the total population retrieved from the SSP database developed by the International Institute for Applied Systems Analysis (IIASA) and the National Center for Atmospheric Research (NCAR) (Riahi et al., 2017; Samir and Lutz, 2017) for each country. The raster of nation-states was retrieved from the Gridded Population of the World, Version 4 (GPWv4): National Identifier Grid (Center for International Earth Science Information Network (CIESIN) - Columbia University, 2018) and is used to aggregate the calculated mortality to country-level mortality estimates. We further categorize the world into 21 regions following the Global Burden of Disease (GBD) Study based on epidemiological similarities and geographic proximity.

Other studies estimating air pollution-related mortality have typically calculated mortality uncertainty based on the confidence intervals (CIs) of the parameters used in the attributable fraction (AF) calculations (Peng et al., 2021; Eastham et al., 2018). However, less attention has been given to the uncertainty arising from internal model variability. Internal variability can

https://doi.org/10.5194/egusphere-2025-3151
Preprint. Discussion started: 30 July 2025

drive regional air quality differences (Fiore et al., 2015). Thus, we focus on the uncertainty associated with ensemble spread and therefore use only the central estimate for β (for ozone) and RR (for $PM_{2.5}$).

3 Results

3.1 Changes in health-related air pollutants

In Fig. 1, and in the subsequent mortality analysis, we present changes in surface $PM_{2.5}$, ozone, temperature (T_s), and total precipitation in three ways: (1) the 2060–2069 average from the ARISE-SAI-1.5 simulation minus 2030-2039 average from SSP2-4.5, illustrating the change under SAI implementation; (2) the 2060–2069 average from SSP2-4.5 minus 2030-2039 average from SSP2-4.5, representing changes under the SSP2-4.5 pathway without SAI; and (3) the difference between the 2060–2069 averages of the ARISE-SAI-1.5 simulation and SSP2-4.5, showing the direct impact of SAI by comparing a future with SAI to one without. Particularly when looking at air quality impact, these three-way comparison is of particular relevance as we generally expect a reduction in surface pollutants in future scenarios independently of SAI implementation, therefore a comparison just between the present day and future SAI scenario will almost always indicate improved air quality. Therefore, comparing also the same future periods (which have the same surface emissions) with and without SAI helps to isolate the direct SAI contribution to air quality.

Consistent with previous studies (Visioni et al., 2023), ARISE-SAI-1.5 exhibits notable regional shifts in precipitation relative to SSP2-4.5 (Fig. 1f) associated with changes in the strength and position of the Intertropical Convergence Zone (ITCZ) and the Hadley circulation (Kravitz et al., 2017; Lee et al., 2020; Richter et al., 2022; Cheng et al., 2022). While some regions do not exhibit statistically significant changes in surface $PM_{2.5}$ relative to SSP2-4.5 (2030–2039), other areas - such as Central America and central Sub-Saharan Africa - do show significant reductions. In these regions, $PM_{2.5}$ decreases coincide with increases in precipitation (Fig. 1d–f), suggesting that enhanced wet scavenging may play a role. However, the overall spatial pattern of $PM_{2.5}$ changes does not consistently align with precipitation trends (Fig. 1g, h and j), indicating that other processes, such as changes in circulation, vertical mixing, or aerosol-cloud interactions, may also contribute to changes in $PM_{2.5}$. Thus, while precipitation influences $PM_{2.5}$ in some regions, it does not fully explain the simulated patterns or their statistical significance.

Furthermore, Fig. 2 indicates that dust and secondary organic aerosols (SOA), rather than sulfate (SO_4), are the dominant contributors to total $PM_{2.5}$ concentrations across most regions in ARISE-SAI-1.5. In SSP2-4.5 (not shown), the spatial distribution of the dominant $PM_{2.5}$ species is broadly similar, with SO_4 not emerging as the dominant species across most regions. While it is true that sulfate can still drive relative changes in $PM_{2.5}$ even when not dominant in absolute terms, our subsequent analysis of mortality (Section 3.2) shows that the changes in $PM_{2.5}$ concentrations and $PM_{2.5}$-related mortality are not driven by sulfate. Specifically, the spatial and temporal patterns of $PM_{2.5}$-related mortality changes align more closely with changes in non-sulfate species and are shaped by precipitation and circulation-driven effects such as wet scavenging and regional aerosol transport.

https://doi.org/10.5194/egusphere-2025-3151
Preprint. Discussion started: 30 July 2025

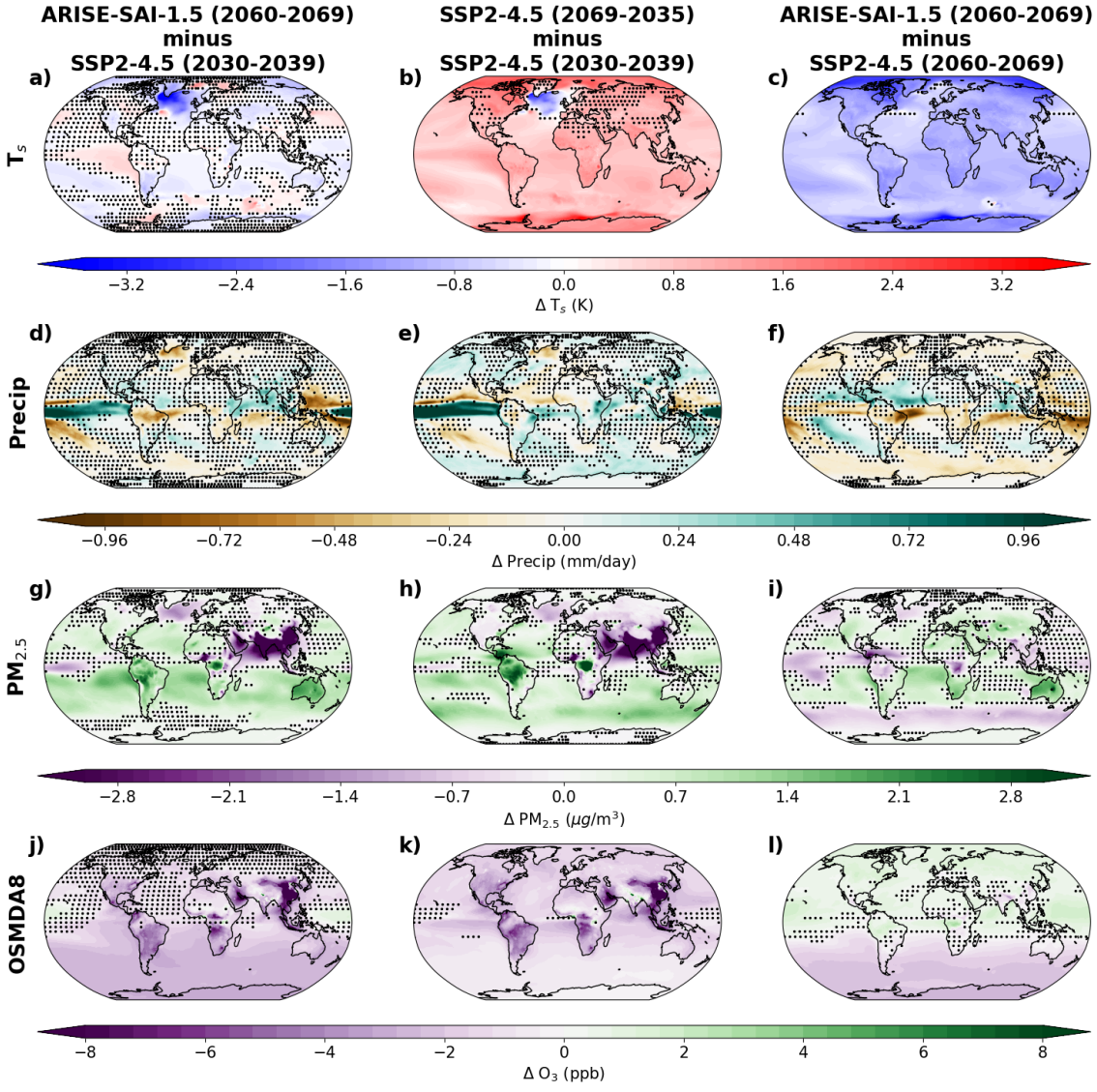

Figure 1. Spatial patterns of the changes in surface climate variables (surface temperature and precipitation) and air quality ($PM_{2.5}$ and ozone exposure (OSMDA8) concentration) under the SAI scenario, ARISE-SAI-1.5, and the baseline scenario (SSP2-4.5). Each row represents changes in: (a-c) surface temperature (T_s, K), (d-f) precipitation (mm/day), (g-i) $PM_{2.5}$ concentration ($\mu g/m^3$), and (j-1) OSMDA8 (ppb). The stippling indicates areas where differences between ARISE-SAI-1.5 and SSP2-4.5 are not statistically significant ($p>0.05$) based on a t-test performed across all 10 ensemble members. Columns indicate the difference between the SAI case and the reference period with same global temperatures (left), the difference between a warmer future and the reference period (center), and the difference between the SAI case and a warmed future following the same underlying emission scenario (right).

https://doi.org/10.5194/egusphere-2025-3151
Preprint. Discussion started: 30 July 2025

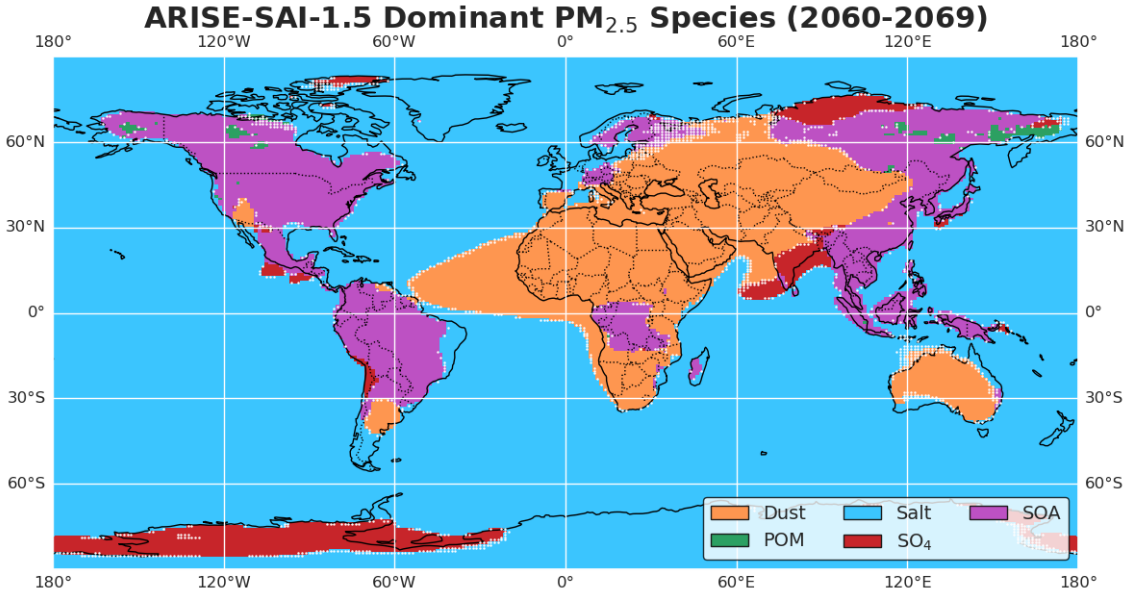

Figure 2. Map of the most prevalent $PM_{2.5}$ species (dust, primary organic matter (pom), salt, sulfate (SO_4), secondary organic aerosols (SOA) and black carbon (BC)) across grid cells, derived from ensemble model averages. Colors represent the dominant species at each location, determined by taking the fraction of the species to the total $PM_{2.5}$ concentration. Note that black carbon is not presented here because it does not dominate in any grid cell. White stippling are over areas where fewer than 90% of ensemble members agree on the dominant species at a grid point.

Lastly, Fig. 1j-l shows changes in surface ozone exposure. Interpreting these changes requires accounting for multiple mechanisms, including SAI-induced impacts on stratospheric ozone and its transport to the surface, and changes in ozone in-situ photochemical processing driven by changes in temperature and photolysis. We note that our study does not include tropospheric ozone changes caused by changes in photolysis, as in the troposphere photolysis rates are fixed at the present-day levels. SAI influences stratospheric ozone through multiple pathways, including alterations in heterogeneous chemical reactions on aerosol surfaces, modifications in photolysis rates due to changes in stratospheric radiation, and dynamical changes in stratospheric circulation and temperature patterns that can impact ozone transport and distribution (Tilmes et al., 2009, 2022; Bednarz et al., 2023a). Injection strategy also plays a key role: in ARISE-SAI-1.5, SO_2 is injected primarily in the Southern Hemisphere during 2060–2069 to modulate hemispheric temperature gradients, resulting in an asymmetric stratospheric aerosol burden and consequently an asymmetric ozone response (Richter et al., 2022; Bednarz et al., 2023b).

This stratospheric asymmetry propagates to the troposphere. Specifically, ozone concentrations decrease across much of the Southern Hemisphere troposphere, while increasing in the Northern Hemisphere (Fig. 1l; Fig. 3f). These hemispheric differences arise from distinct underlying mechanisms. In the Southern Hemisphere, the reduction in surface ozone is primarily driven by the reductions in stratospheric ozone concentrations in the SH mid and high latitudes under aerosol-driven catalytic

https://doi.org/10.5194/egusphere-2025-3151
Preprint. Discussion started: 30 July 2025

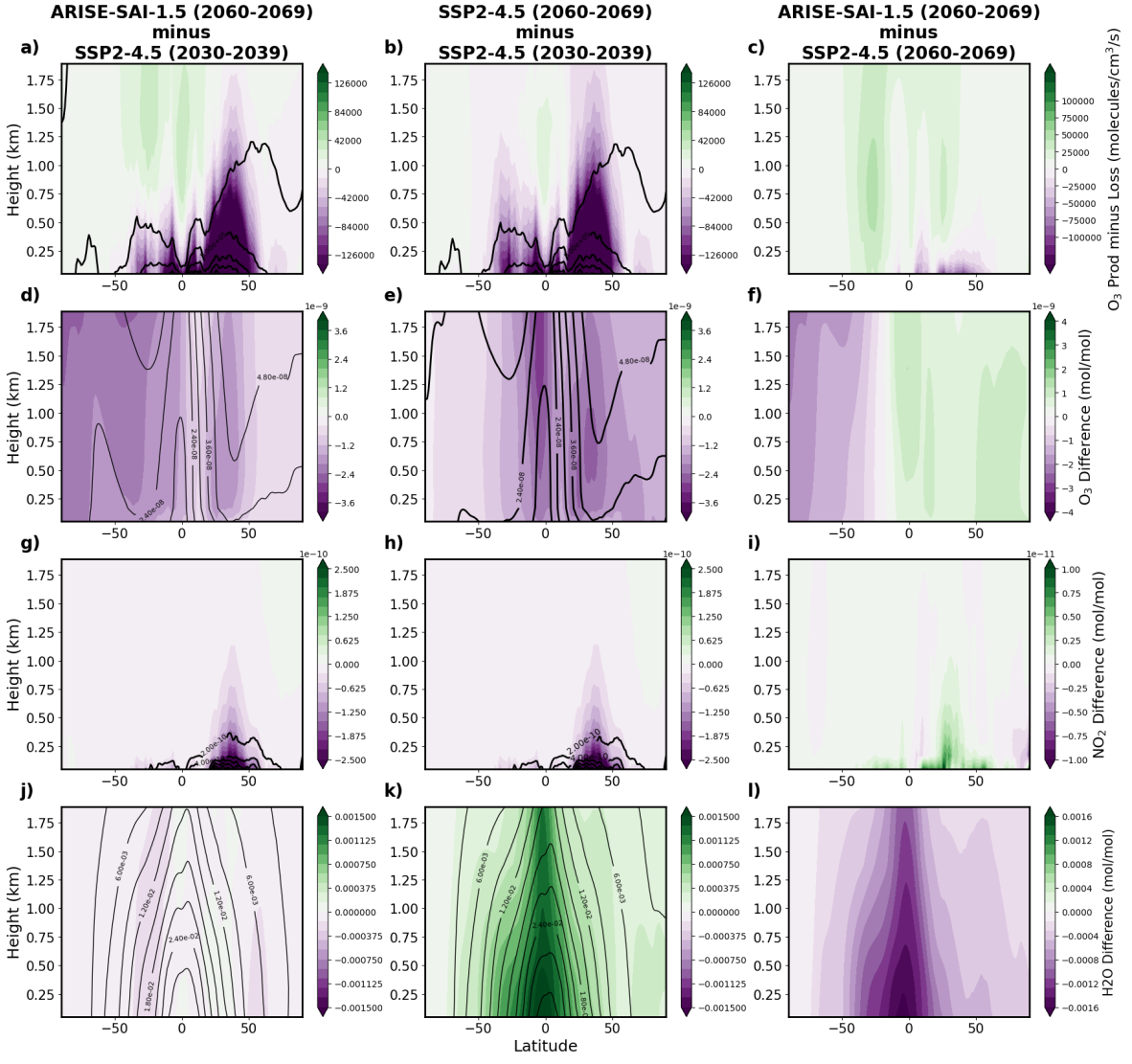

Figure 3. Zonal-mean changes in ozone chemical production minus loss rates, ozone concentrations, and NO_2 concentrations under ARISE-SAI-1.5 and SSP2-4.5 scenarios. Panels (a–c) show the difference in ozone production minus loss (molecules cm^{-3} s^{-1}): (a) ARISE-SAI-1.5 (2060–2069) minus SSP2-4.5 (2030–2039), (b) SSP2-4.5 (2060–2069) minus SSP2-4.5 (2030–2039), and (c) ARISE-SAI-1.5 (2060–2069) minus SSP2-4.5 (2060–2069). Panels (d–f) show the corresponding differences in ozone concentrations (mol mol^{-1}) for the same scenario comparisons. Panels (g–i) show differences in NO_2 concentrations (mol mol^{-1}), highlighting changes in a key ozone precursor and panels (j-l) show differences in H_2O concentrations. In each panel, shading denotes the magnitude of the difference, and black contours indicate the absolute zonal-mean values from the first dataset of each comparison (e.g., ARISE-SAI-1.5 or SSP2-4.5).

195 ozone loss in the Antarctic stratosphere alongside any changes in polar vortex strength and large-scale stratospheric transport (Bednarz et al., 2023b), and the resulting reduction in STE.

https://doi.org/10.5194/egusphere-2025-3151
Preprint. Discussion started: 30 July 2025

In contrast, the Northern Hemisphere surface ozone increases are likely not driven by changes in STE. Although stratospheric ozone increases occur in the NH lower-to-mid stratosphere (Fig. A4), this signal does not extend to the surface. Hence, the NH surface ozone changes likely reflect the SAI-induced changes in in-situ tropospheric chemical processing. In particular, H2O levels decrease throughout the troposphere in ARISE-SAI-1.5 compared to SSP2-4.5 (Fig. 3l) as the result of large scale near-surface cooling (Fig. 1c). This reduces chemical ozone loss in the free-troposphere, as indicated by an increased net photochemical ozone production (Fig. 3c). Owing to rapid tropospheric mixing timescales, the resulting NH ozone increases extend to the surface, even despite negative (particularly between 0 to 50°N) NH surface net production changes under SAI. The latter indicate suppressed in-situ photochemical ozone formation that occurs in a NO_x-rich region (see contours in Fig. 3g,h and Fig. A5) under decreased OH (Fig. A6) and the resulting suppressed RO2-NO2 cycling (despite a concurrent increase in NH surface NO_x which should otherwise enhance ozone production , Fig. 3i), consistent with previous work demonstrating that reductions in temperature and humidity can suppress photochemical ozone formation in NO_x-rich environments Archibald et al. (2020); Rasmussen et al. (2013); Doherty et al. (2013); Zanis et al. (2022).

To further test this interpretation, we repeated our analyses in simulations with simulated SAI injections but no changes in tropospheric anthropogenic emissions (i.e. in a preindustrial climate) and observed qualitatively similar ozone responses, reinforcing our finding that the changes arises from stratospheric chemistry, transport, and in-situ oxidant perturbations, consistent with previous findings on SAI-driven ozone redistribution (e.g., Xia et al., 2017; Niemeier and Schmidt, 2017; Tilmes et al., 2009).

3.2 Calculation of the air pollution related mortality from $PM_{2.5}$ and ozone changes

This section presents the estimated mortality impacts of SAI under the ARISE-SAI-1.5 protocol, relative to SSP2-4.5. We include the 35-year ARISE-SAI-1.0 simulation in Fig. 7 and 8.

We first examine changes in $PM_{2.5}$ resulting from SAI, followed by an assessment of ozone-related mortality. Together with showing ensemble-averaged results, we also highlight in the following maps the large inter-ensemble and inter-ensemble spread when calculating mortality based on yearly model output. Local air quality is strongly dependent on meteorological conditions (Liu et al., 2022; Jacob and Winner, 2009; Xu et al., 2020) such as precipitation rates, heatwaves and atmospheric inversion. Global warming itself has been postulated to strengthen many of this conditions as well (Jacob and Winner, 2009). Therefore, we deem important to place our obtained average estimates in this context.

Fig. 4 and 7a show the annual global deaths resulting from changes in $PM_{2.5}$ concentration and the average $PM_{2.5}$-related deaths by country, respectively. We estimate that SAI leads to a reduction of 151,750 premature deaths from $PM_{2.5}$ under ARISE-SAI-1.5 (2060-2069), relative to SSP2-4.5 (2030-2039), with ensemble member estimates ranging from -140,245 to -164,068. In comparison, SSP2-4.5 (2060-2069) results in a reduction of 165,669 premature deaths relative to 2030-2039 levels, with a range of -148,397 to -177,296. This yields a net increase of 13,918 premature deaths in ARISE-SAI-1.5 compared to SSP2-4.5 during 2060-2069, with an ensemble range of -7,468 to +21,177. These estimates and Fig. 4 show that the standard deviation of mortality estimates highlights the large spread in projected $PM_{2.5}$-related deaths.

https://doi.org/10.5194/egusphere-2025-3151
Preprint. Discussion started: 30 July 2025

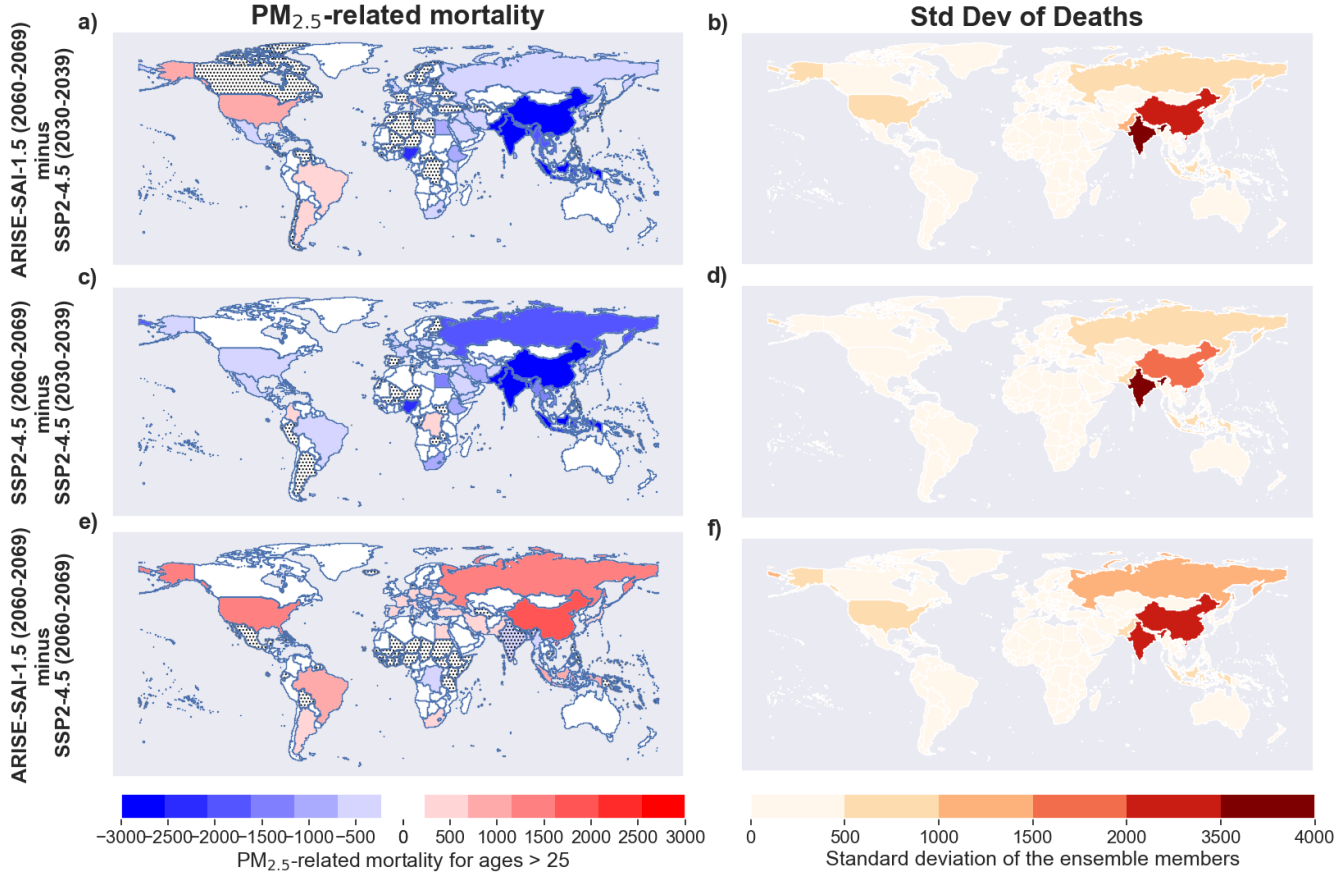

Figure 4. The ensemble-mean deaths from $PM_{2.5}$ for ages > 25. Stippling indicates countries where changes are not statistically significant ($p>0.05$) based on a two-sided t-test across ensemble members.

The changes in $PM_{2.5}$-related mortality for each country in Fig. 4e are roughly consistent with the geographical changes in $PM_{2.5}$ shown in Fig. 1i. In Fig. 5a, we compute the ensemble-averaged global deaths resulting from SSP2-4.5 with added changes in individual $PM_{2.5}$ components between ARISE-SAI-1.5 and SSP2-4.5 to isolate the influence of each component on global mortality. Among the components, incorporating changes in the dust $PM_{2.5}$ produce the largest deviation from the unmodified SSP2-4.5 baseline. Notably, the scenario with dust-only modifications results in fewer global deaths than the SSP2-4.5 baseline, which is likely due to the nonlinearity in the ozone-attributable risk function (see Fig. A1b). However, when changes in all $PM_{2.5}$ components are combined, the resulting mortality aligns with the increased PM2.5-related mortality observed in ARISE-SAI-1.5. For other components such as salt, BC, POM, SOA and SO_4, the resulting mortality estimates largely overlap the unmodified SSP2-4.5 baseline. In particular, the changes in global deaths attributable to SO_4 are relatively small, implying that sulfate-driven $PM_{2.5}$ mortality changes are modest compared to the total. Therefore, SAI's contribution to $PM_{2.5}$–related mortality appears small, with internal variability among ensemble members and changes from other $PM_{2.5}$–

https://doi.org/10.5194/egusphere-2025-3151
Preprint. Discussion started: 30 July 2025

related species, potentially driven by precipitation changes, playing a dominant role in driving uncertainty in our mortality estimates.

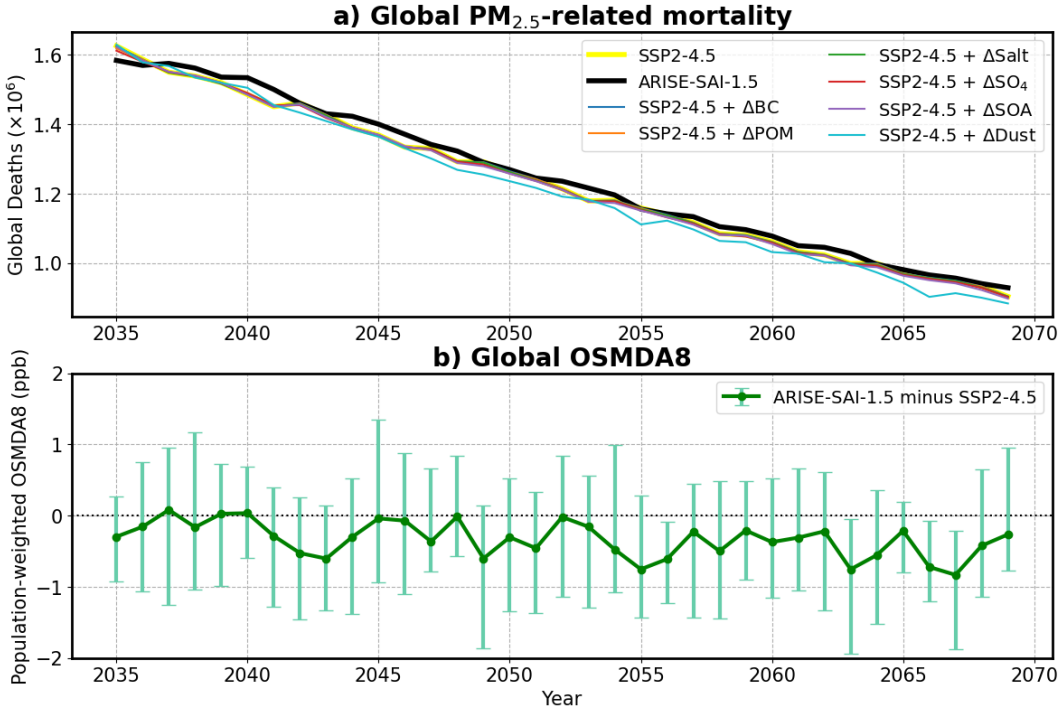

Figure 5. (a) Ensemble-averaged global $PM_{2.5}$-related mortality over time under the SSP2-4.5 and ARISE-SAI-1.5 scenarios, along with sensitivity simulations where changes in individual $PM_{2.5}$ components (ΔBC, ΔPOM, ΔSalt, ΔSO_4, ΔSOA, ΔDust) between ARISE-SAI-1.5 and SSP2-4.5 are added to the SSP2-4.5 baseline. (b) Time series of population-weighted global OSMDA8 (daily maximum 8-hour ozone) differences between ARISE-SAI-1.5 and SSP2-4.5, with error bars indicating ensemble spread ($\pm$ 1 standard deviation).

For ozone-related mortality, Fig. 7b and 6 show the annual global total deaths resulting from changes in ozone concentration and the average ozone-related deaths by country, respectively. We estimate that SAI leads to a reduction of 101,706 premature deaths from ozone exposure under ARISE-SAI-1.5 (2060–2069), relative to SSP2-4.5 (2030–2039), with an ensemble range of -91,413 to -108,493. By comparison, SSP2-4.5 (2060-2069) results in an estimated reduction of 87,819 premature deaths from ozone exposure relative to SSP2-4.5 for 2030–2039, with a range of -76,583 to -96,917. The net difference between ARISE-SAI-1.5 and SSP2-4.5 during 2060-2069 is -13,887, with a range of -6,610 to -24,852. Fig. 6 shows that the standard deviation of the ozone-related mortality is smaller than that of $PM_{2.5}$-related mortality globally, indicating lower ensemble variability.

The geographic distribution of ozone-related mortality changes, shown in Fig. 6, indicates that mortality reductions are concentrated primarily in Southeastern Asia. This spatial pattern aligns with the hemispheric asymmetry in the tropospheric ozone response observed in Fig. 3, where greater reductions in ozone concentrations occur in the Southern Hemisphere and parts of Asia.

https://doi.org/10.5194/egusphere-2025-3151
Preprint. Discussion started: 30 July 2025

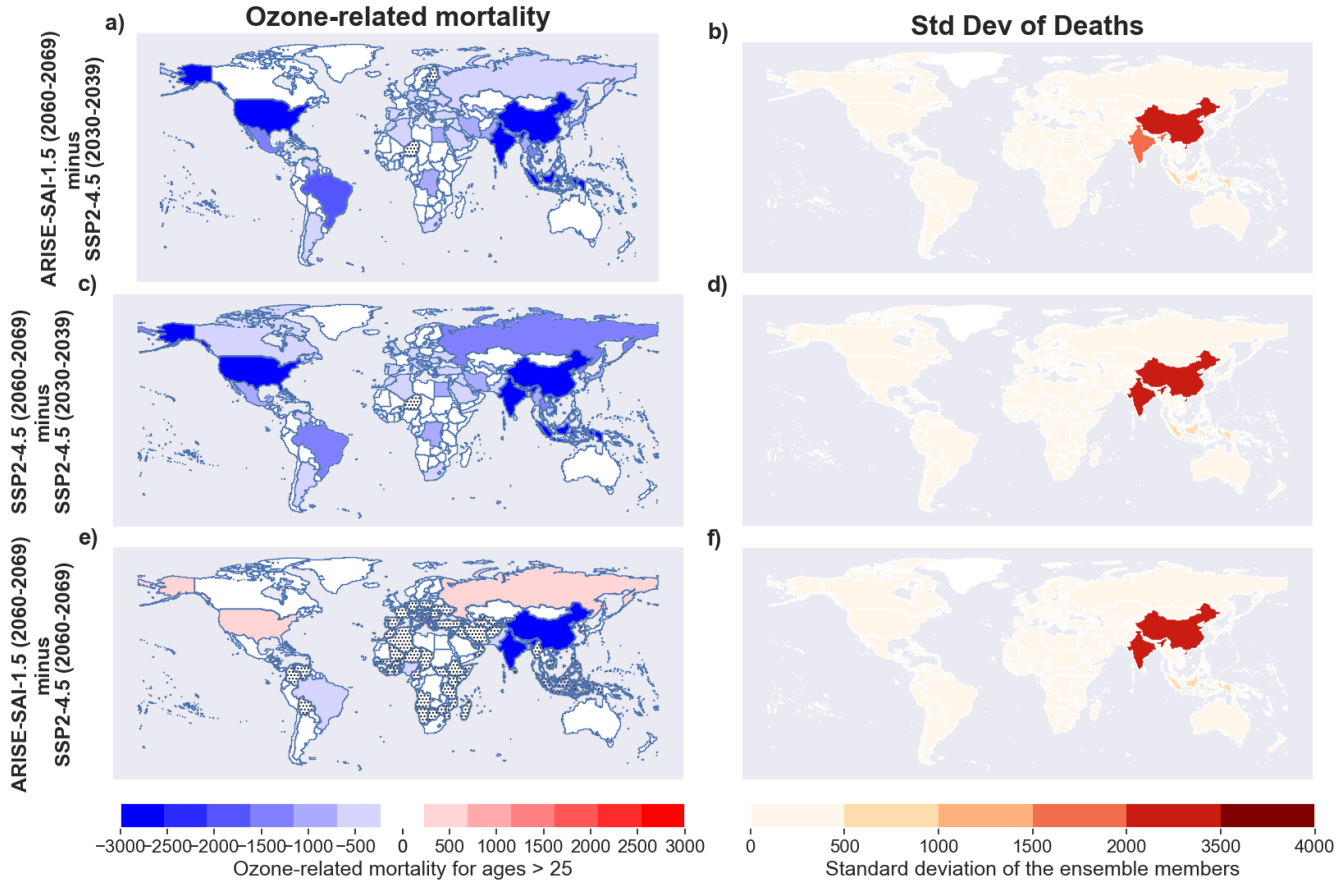

Figure 6. The ensemble-mean deaths from ozone for ages $>$ 25. Stippling indicates countries where changes are not statistically significant ($p>0.05$) based on a two-sided t-test across ensemble members.

For both ozone and $PM_{2.5}$-related mortality, the range of total global deaths resulting from changes in air pollution illustrates the variability across ensemble members and highlights the importance of quantifying the internal variability within a model. The magnitude of these changes varies substantially across all ensemble members, emphasizing the role of internal variability in shaping the projected health impacts. Furthermore, the geographical distribution of the changes in ozone and $PM_{2.5}$-related mortality reflect that the regional health benefits of SAI implementation are not uniform, but instead reflect underlying patterns in how surface air pollution responds to stratospheric aerosol perturbations. Both ozone-and $PM_{2.5}$-related mortality changes exhibit substantial spatial variability, driven by regional differences in how ozone and $PM_{2.5}$ concentrations respond to shifts in atmospheric chemistry, circulation, and precipitation patterns under SAI.

Figure 7 shows how global changes in mortality due to ozone and $PM_{2.5}$ evolve over time in our simulations. When aggregated globally, it is evident that the largest change is due to decreases in precursors and pollutants under the SSP2-4.5 scenario. The differences between the futures with and without SAI, and those between different amount of SAI cooling, are

https://doi.org/10.5194/egusphere-2025-3151
Preprint. Discussion started: 30 July 2025

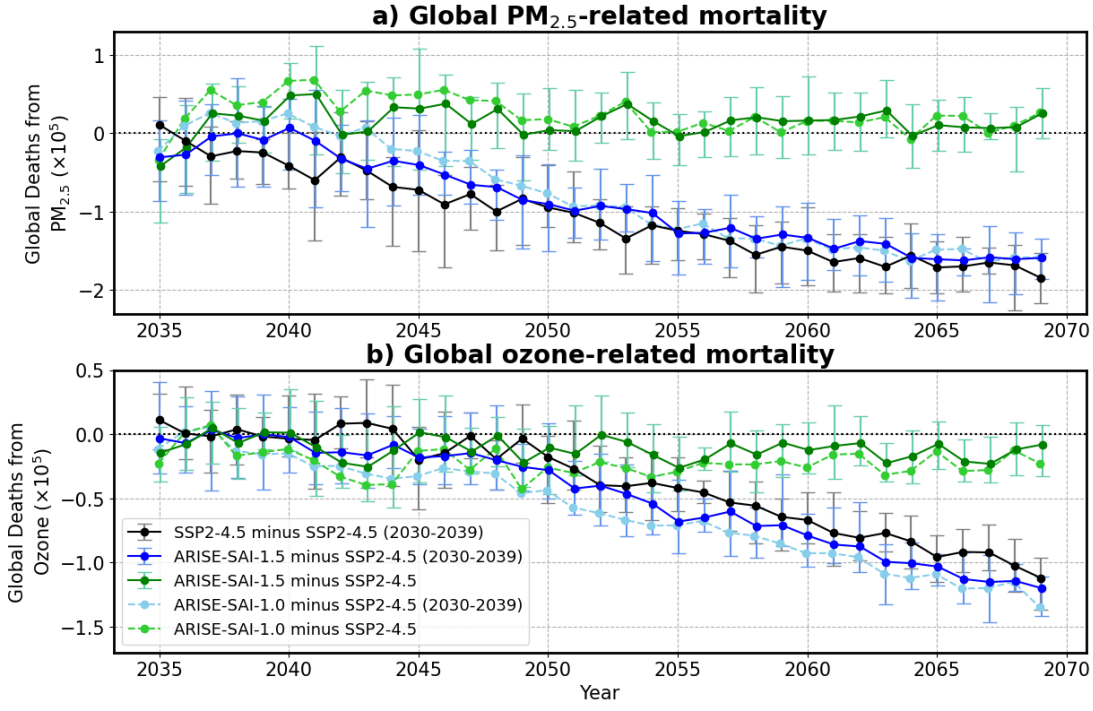

Figure 7. Global deaths from a) $PM_{2.5}$ and b) ozone evaluated as 1) ARISE-SAI-1.O minus SSP2-4.5, 2) ARISE-SAI-1.5 minus SSP2-4.5 (2030-2039), 3) ARISE-SAI-1.5 minus SSP2-4.5, 4) SSP2-4.5 minus SSP2-4.5 (2030-3029) and 5) ARISE-SAI-1.5 minus SSP2-4.5 (2030-2039). Error bars represent the full range of outcomes across the model ensemble, showing the minimum and maximum values.

much smaller on a per-year basis, and in most cases within the range of variability for the ensemble estimates. This clearly demonstrates that the direct impact of deposited sulfate is almost null, whereas climatic factors only minimally impact PM2.5 changes under SAI. In contrast, ozone-attributable mortality is lower in ARISE-SAI-1.0, likely due to enhanced cooling that reduced OH concentrations, thereby suppressing tropospheric ozone production.

Figure 8 presents an alternative way of examining this relationship by plotting ensemble means from ARISE-SAI-1.0 and ARISE-SAI-1.5 against their respective injection rates, rather than as a time evolution. For both simulations, $PM_{2.5}$-related mortality exhibits a weakly positive trend with increasing injection rates. However, substantial ensemble variability, represented by the error bars, reflects considerable ensemble member spread in the mortality response. In contrast, ozone-attributable mortality remains consistently negative across the entire injection range, indicating a reduction in ozone-related deaths under both ARISE-SAI-1.5 and ARISE-SAI-1.0. These results reveal that pollution-driven mortality under SAI does not scale linearly or even monotonically with the amount of SO_2 injected into the stratosphere. With the injection of SO_2 into the stratosphere, the resulting atmospheric responses involve complex feedbacks that we have tried to outline in this manuscript.

For $PM_{2.5}$-related mortality in particular, our component attribution analysis suggests that the primary driver of changes is not sulfate itself, but rather arising from changes in dust and secondary SOA concentrations. Regional reductions in $PM_{2.5}$,

https://doi.org/10.5194/egusphere-2025-3151
Preprint. Discussion started: 30 July 2025

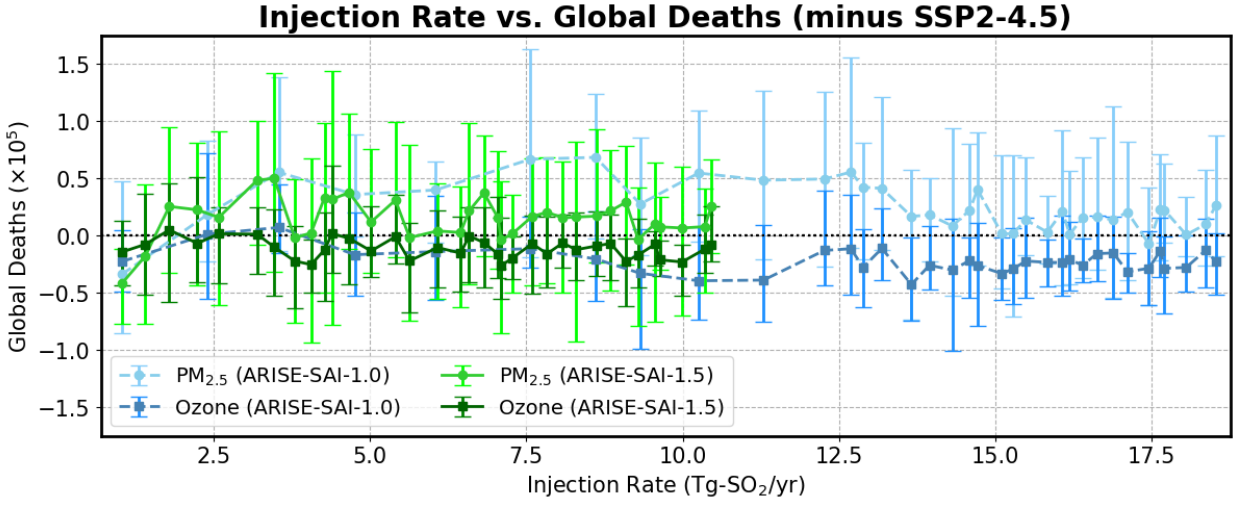

Figure 8. Global mortality differences for ARISE-SAI-1.5 minus SSP2-4.5 (shades of green) and ARISE-SAI-1.0 minus SSP2-4.5 (shades of blue) as a function of annual SO_2 injection rate (Tg-SO_2/yr), for $PM_{2.5}$-related deaths (green) and ozone-related deaths (green). Points represent ensemble means across years (2035–2069), with error bars indicating ensemble variability (± 1 standard deviation).

particularly over Central America and central Sub-Saharan Africa, align with areas of increased precipitation, highlighting the role of wet deposition and circulation-driven suppression of natural aerosol sources. However, the widespread lack of statistically significant precipitation or $PM_{2.5}$ changes across ensemble members suggests that internal variability and regional circulation shifts, rather than sulfate burden alone, govern the spatial and temporal patterns of $PM_{2.5}$-related health outcomes under SAI.

For ozone, the mortality reductions appear more discernible. SO_2 is primarily injected in the Southern Hemisphere, leading to decreased SH extra-tropical lower stratospheric ozone concentrations and the resulting reduction in SH surface ozone from reduced STE overwhelming any in-situ changes in tropospheric ozone chemistry there. In the Northern Hemisphere, on the other hand, surface ozone increases due to the suppressed photochemical destruction under drier and colder troposphere. These changes reflect the role of not only hemispheric asymmetries in sulfate burden alone but also those in STE and chemical processing arising from circulation changes and altered chemical regimes in shaping global ozone responses and associated health outcomes under SAI.

Taken together, these findings emphasize that air pollution-related health impacts under SAI are not governed mainly by the magnitude of SO_2 injected, but rather by the complex suite of dynamical, chemical, and aerosol responses in the Earth system–many of which are nonlinear and strongly influenced by internal variability.

https://doi.org/10.5194/egusphere-2025-3151
Preprint. Discussion started: 30 July 2025

3.3 GBD super-region specific projections

Globally, ARISE-SAI-1.5 reduces total pollution-attributable mortality relative to a future without intervention (SSP2-4.5) by 0.41%, driven by a 0.86% increase in $PM_{2.5}$ and 1.26% reduction in ozone-related deaths (Fig. 9a–b). However, the direction and magnitude of health outcomes vary substantially across GBD super-regions. For instance, large percent increases in $PM_{2.5}$-related mortality occur in regions such as Central, Western and Eastern Europe. In contrast, regions like the Caribbean and Central Latin America exhibit reductions in $PM_{2.5}$-attributable mortality–highlighting the heterogeneous and sometimes adverse regional impacts of SAI.

For ozone-related mortality, the ensemble spread is also large—both in magnitude and spatial extent—especially in regions such as the Western and Eastern Sub-Saharan Africa and the Caribbean. Furthermore, while BMR (cardiovascular, respiratory, and NCD+LRI baseline mortality rate) declines from 2030–2039 to 2060–2069 across all regions (see Appendix), the magnitude of these changes is relatively small compared to the much larger shifts seen in air quality-related mortality.

In many regions, the direction of the response varies across ensemble members, reflecting uncertainty not only in the scale but also in the sign of the projected impact. This spread arises from internal climate variability, which influences key drivers of air quality–such as atmospheric circulation, precipitation patterns, and chemical processing–and leads to diverging pollutant concentrations across ensemble members, even under identical forcing scenarios. These findings also highlight the spatial heterogeneity in health responses to SAI. While global or hemispheric trends may point to a net decline in ozone-related mortality and an increase in $PM_{2.5}$-related mortality, such aggregates can mask substantial regional disparities. As a result, careful evaluation of region-specific trade-offs is critical when assessing the overall public health implications of SAI deployment.

4 Conclusions

This study evaluates the impacts of SAI on air quality–related mortality using a fully coupled climate model ensemble under the ARISE-SAI protocol. Unlike previous studies using CTMs (e.g., Eastham et al. 2018; Moch et al. 2023), which imposed stratospheric aerosols without capturing feedbacks on dynamics and transport, our use of CESM2-WACCM6 enables interactive coupling between aerosols, chemistry, and climate. Our main finding is that the potential effects of SAI on surface air quality and associated mortality are relatively modest and largely fall within the range of internal model variability. In particular, pollution-related mortality are reduced by 18.2% in SSP2-4.5 compared to present day due to air quality policies, and by 18.6% in ARISE-SAI-1.5 due to the combination of air quality policies and SAI contributions, underscoring the importance of public policies that are having and will have large capacity to improve health outcomes (Vandyck et al., 2018).

We explore two potential sources of mortality: $PM_{2.5}$ and surface ozone exposure. $PM_{2.5}$ is affected both by direct deposition of sulfate from the stratosphere and by climatic conditions affecting other sources of particulates. Tropospheric O_3 changes from SAI can be driven by the combination of changes in stratospheric ozone and its transport to the troposphere, and by in-situ changes in tropospheric ozone chemistry driven by SAI-induced changes in temperatures and UV photolysis. We note the latter are not considered in our study, as tropospheric photolysis rates are fixed in the model at the present day levels.

https://doi.org/10.5194/egusphere-2025-3151
Preprint. Discussion started: 30 July 2025

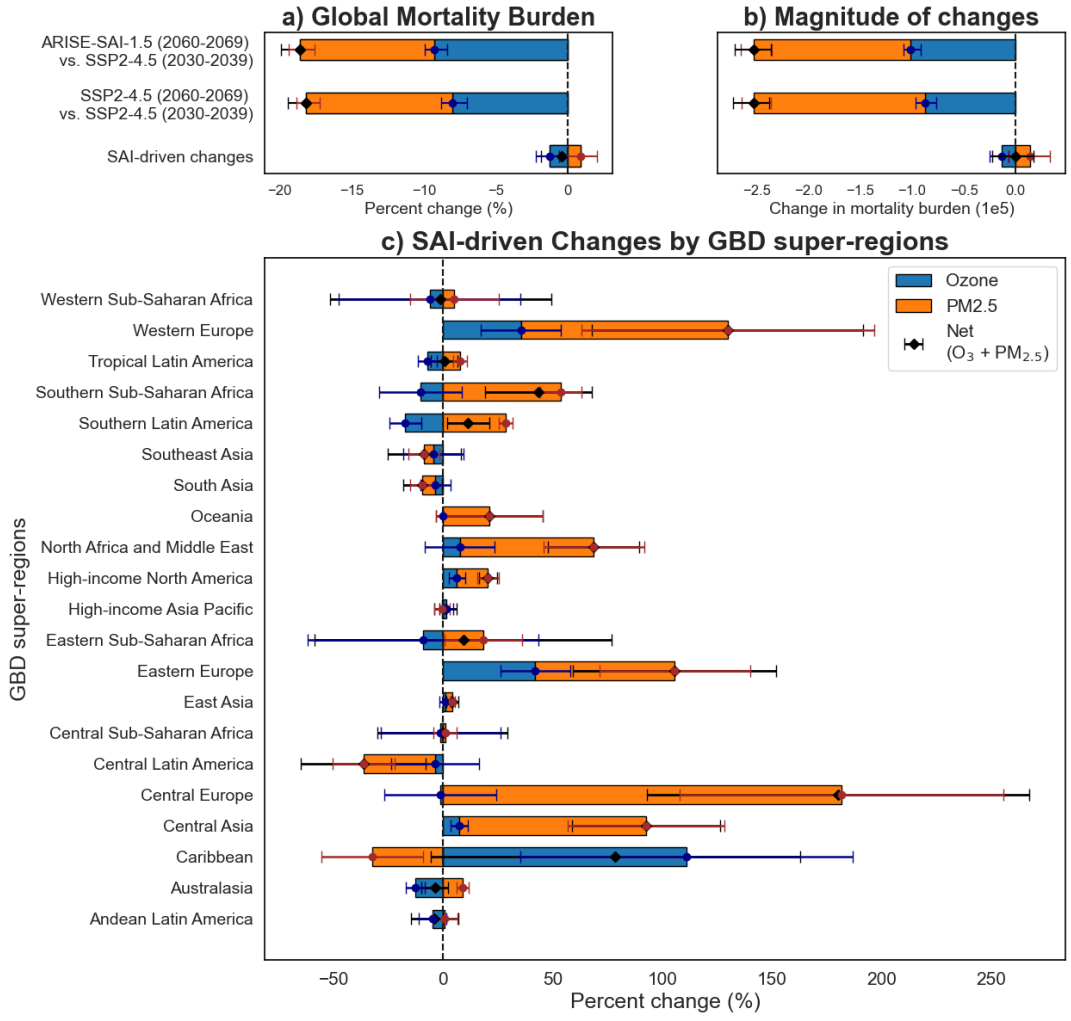

Figure 9. (a) Global percent change in mortality burden comparing ARISE-SAI-1.5 (2060–2069) and SSP2-4.5 (2030–2039), as well as SSP2-4.5 (2060–2069) and SSP2-4.5 (2030–2039). (b) Absolute global changes in mortality burden (in number of deaths). (c) Percent change in mortality burden by Global Burden of Disease (GBD) super-region between ARISE-SAI-1.5 (2060-2069) and SSP2-4.5 (2060-2069). Percent changes are calculated relative to baseline mortality rates. Positive values indicate an increase in mortality relative to the baseline, while negative values indicate reductions. Bars represent stacked contributions from ozone-related deaths (blue) and $PM_{2.5}$-related deaths (orange), with horizontal error bars indicating the ensemble spread (standard deviation) for each component and for the net total (black diamonds with error bars).

We find the direct contribution of sulfate aerosols to $PM_{2.5}$-related mortality is minimal, primarily because much of the injected sulfate is transported poleward, deposited at midlatitudes, leading to a relatively diffuse and spatially uniform distribution. Furthermore, a portion of sulfate particles exceed the $PM_{2.5}$ size threshold and therefore does not contribute to fine

https://doi.org/10.5194/egusphere-2025-3151
Preprint. Discussion started: 30 July 2025

particulate mass. Subsequently, the total mass of sulfate aerosols reaching the surface is insufficient to meaningfully alter concentration thresholds associated with mortality outcomes. Instead, regional changes in $PM_{2.5}$ concentrations and the corresponding health impacts are mainly driven by shifts in precipitation patterns or circulation, which affect the wet removal of non-sulfate species such as dust and secondary organic aerosols, consistent with Eastham et al. (2018).

Likewise, we find that ozone-related mortality is projected to maintain its decrease globally due to changes in pollutant sources even under SAI; but, when comparing the two future scenarios, the SAI impact result in a change in the spatial pattern reflecting a hemispheric asymmetry in the tropospheric ozone response, leading to a slight increase in surface ozone in the Northern Hemisphere and a decrease in the Southern Hemisphere.

However, some uncertainties related to the specific evolution of surface ozone remain, particularly due to the absence of interactive photolysis in the troposphere, which could lead to an underestimation of chemical feedbacks involving ozone and hydroxyl radicals. In reality, stratospheric aerosols alter the spectral distribution of solar radiation, affecting both the amount and quality of light reaching the lower atmosphere. While SAI increases aerosol optical depth and reduces shortwave radiation (∼400–850 nm), catalytic ozone depletion allows greater transmission of ultraviolet (UV) radiation at wavelengths below 345 nm (Moch et al., 2023). This enhanced UV flux accelerates ozone photolysis ($O_3 + h\nu \rightarrow O_2 + O(^1D)$) and triggers chemical feedbacks that can influence surface ozone and oxidant levels, including increased production of hydroxyl radicals (OH), the primary sink of methane (CH_4). These chemical feedbacks linking photolysis, ozone, OH, and CH_4 are omitted in simulations without interactive photolysis, limiting our ability to capture the full extent of surface ozone responses and oxidant perturbations under geoengineering. Nevertheless, studies including interactive tropospheric photolysis like Moch et al. (2023) do not show a particularly large impact from its inclusion on surface ozone concentrations.

There are other factors that might lead us to different estimates of both $PM_{2.5}$ and ozone-related mortality rates. All mortality estimates in future scenarios are calculated using the fixed 2020 population distribution. This approach isolates the effects of air quality changes by removing confounding influences from projected population growth or redistribution. However, it is important to note that mortality rates could be significantly affected by demographic and population changes, such as aging, urbanization, or overall population growth, which are not considered in this study. As a result, our estimates may not fully reflect future health impacts under evolving demographic conditions. Also, while CESM2-WACCM generally performs comparably to other CMIP6 models in simulating surface air pollution (Turnock et al., 2020), it exhibits a high bias in surface ozone relative to TOAR observations and a low bias in surface $PM_{2.5}$ compared to observational datasets.

Furthermore, our analysis is based on a single climate model, and thus the results may be scenario and model-dependent. However, comparisons between ARISE-SAI-1.0 and ARISE-SAI.1.5 indicate that $PM_{2.5}$-related mortality does not increase due to SAI with higher SO_2 injection amounts, whereas ozone-related mortality decreases with higher injection rates due to lower temperatures. This suggests that variability in PM2.5-related mortality may be more strongly influenced by changes in dust or biomass-burning-derived PM2.5 driven by circulation responses to SAI, rather than directly by the total amount of SO_2 injected.

Future assessments of SAI impacts on air quality and related mortality could be improved by multi-model intercomparisons to better constrain the contributions of non-sulfate aerosol species, such as dust, black carbon, and secondary organic aerosols,

https://doi.org/10.5194/egusphere-2025-3151
Preprint. Discussion started: 30 July 2025

as well as to capture the range of model uncertainty in aerosol-chemistry climate interactions. Additionally, improved representation and observational verification of large-scale circulation responses, particularly changes in the Brewer-Dobson Circulation and STE, are essential for understanding the transport and distribution of injected aerosols, as well as their downstream effects on regional air quality. Furthermore, the incorporation of more detailed aerosol microphysics, including size-resolved coagulation, nucleation, and heterogeneous chemistry, would allow for a more accurate simulation of aerosol growth, lifetime, and radiative properties. Together, these efforts would enable more comprehensive and policy-relevant evaluations of SAI's atmospheric and health impacts.

While this study focused on the air quality-related health impacts of SAI, it is important to acknowledge that other health-relevant outcomes, such as changes in surface UV radiation and regional temperature, were not evaluated here but may also carry significant implications. Preliminary analysis of surface UV radiation differences between ARISE-SAI-1.5 and SSP2-4.5 indicate very modest changes and were not included in the manuscript. Like air quality, these impacts are embedded within a broader suite of SAI-induced environmental changes that merit further explorations. Furthermore, internal climate variability plays a critical role in modulating aerosol transport, chemical processes, regional temperature responses, and stratospheric ozone dynamics. By resolving dynamic feedbacks between aerosols, transport, and atmospheric chemistry, our modeling approach overcomes key limitations of earlier CTM-based studies, enabling more realistic estimates of SAI-induced air quality and health outcomes. This highlights the importance of using fully coupled Earth system models when evaluating the policy-relevant consequences of geoengineering strategies and reinforces the need to account for natural variability when assessing human health. Our results, which emphasize the importance of ensemble approaches for air pollution mortality estimates, highlight a general need for robust ensemble-based evaluations across all dimensions of SAI's potential risks and trade-offs.

Code and data availability. Code used in computing the $PM_{2.5}$ and ozone-related mortality can be found at https://doi.org/10.5281/zenodo.15696232 (Wang, 2025). All the data presented in this paper are available at https://doi.org/10.5281/zenodo.6473954 (Richter and Visioni, 2022b) from the CESM2(WACCM6) SSP2–4.5 simulations and at https://doi.org/10.5281/zenodo.6473775 (Richter and Visioni, 2022a) from the ARISE-SAI simulations.

https://doi.org/10.5194/egusphere-2025-3151
Preprint. Discussion started: 30 July 2025

5 Appendix

A comparison of the AF used in this study to calculate $PM_{2.5}$ and ozone associated mortality is presented in Fig. A1. The AF for $PM_{2.5}$ (NCD+LRI) is lower per $\mu g/m^3$ of $PM_{2.5}$ because its harm is spread across many diseases, while ozone's AF is higher per ppb for cardiovascular and respiratory diseases because it acts more acutely and specifically on those systems. In Fig. A1a, $PM_{2.5}$ exhibits a near-linear dose-response relationship with mortality, indicating that risks accumulate gradually. In contrast, Fig. A1b shows that ozone has a steeper curve at lower doses, meaning even small increases in surface O_3 can disproportionately elevate the risk of cardiovascular and respiratory diseases (Burnett and Cohen, 2020).

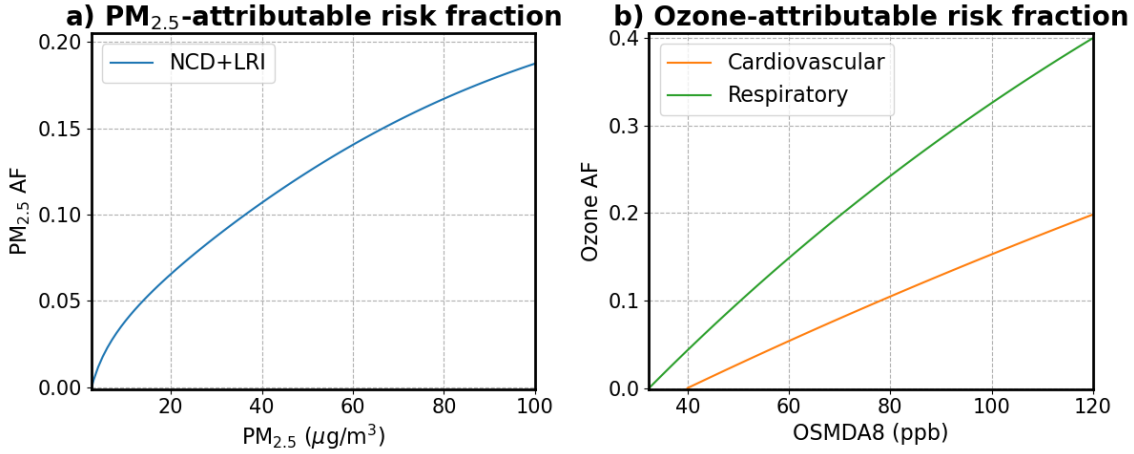

Figure A1. (a) Attributable fraction (AF) of mortality due to PM2.5 exposure as a function of PM2.5 concentration, based on the mean relative risk (RR) across age groups for non-communicable diseases (NCD) and lower respiratory infections (LRI). (b) Attributable fraction of mortality due to ozone (OSMDA8) exposure, with separate curves for cardiovascular and respiratory causes. Risk functions are based on excess mortality relative to baseline thresholds (2.5 ppm for NCD+LRI, 40 ppb for cardiovascular and 32.4 ppb for respiratory outcomes).

https://doi.org/10.5194/egusphere-2025-3151
Preprint. Discussion started: 30 July 2025

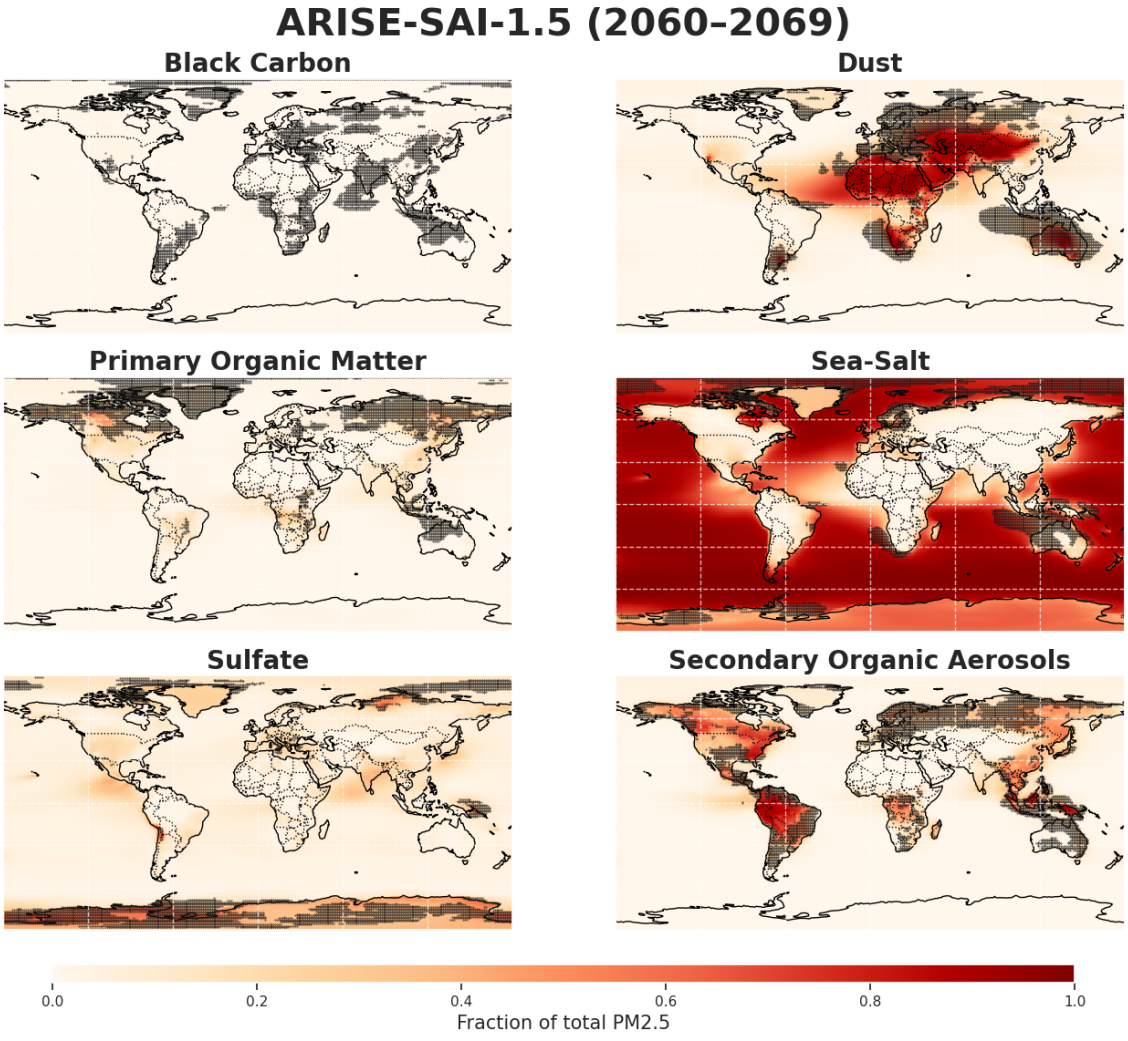

Figure A2. Mean fractional contribution of PM2.5 species under ARISE-SAI-1.5 (2060–2069). Color shading shows the ensemble-mean fraction of each species relative to total PM2.5. Stippling marks regions where the ensemble standard deviation exceeds the 90th percentile, indicating high internal variability.

https://doi.org/10.5194/egusphere-2025-3151
Preprint. Discussion started: 30 July 2025

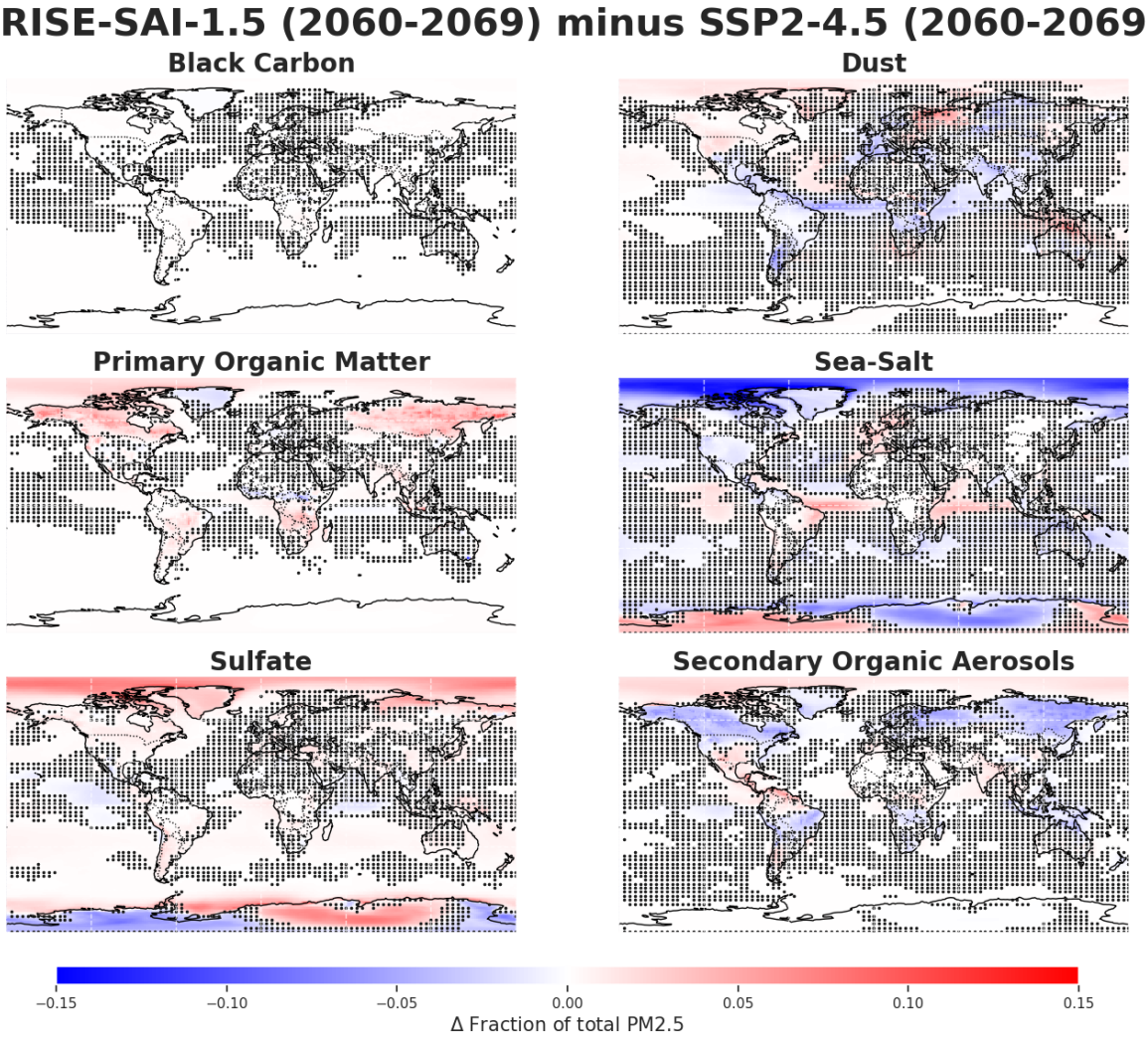

Figure A3. Changes in the fractional contribution of $PM_{2.5}$ species between ARISE-SAI-1.5 and SSP2-4.5 (2060–2069). Positive (red) values indicate an increased contribution under ARISE-SAI-1.5, while negative (blue) values indicate a decreased contribution. Sparse stippling marks areas where changes are not statistically significant ($p>0.05$) based on a two-sided t-test across ensemble members.

https://doi.org/10.5194/egusphere-2025-3151
Preprint. Discussion started: 30 July 2025

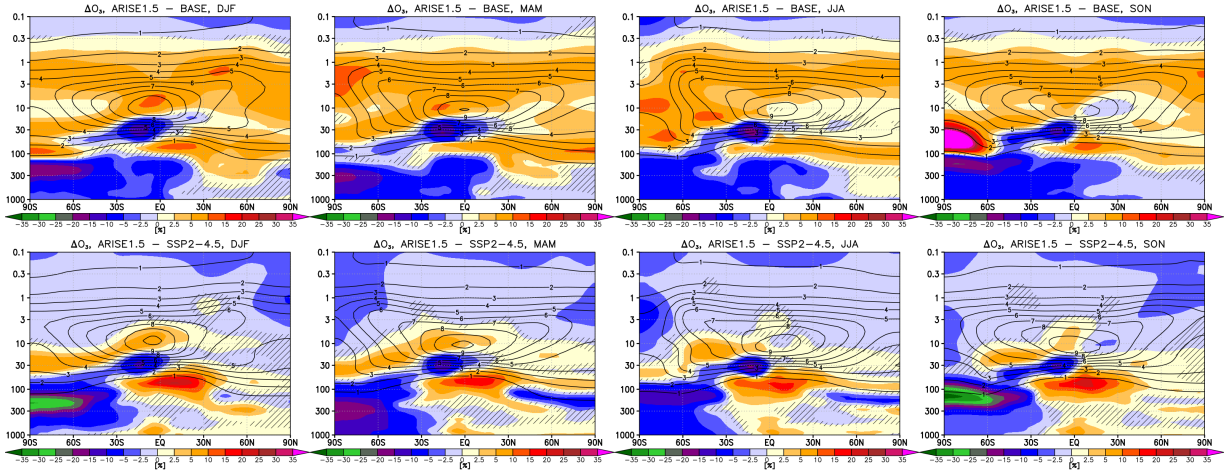

Figure A4. Seasonal changes in ozone between ARISE-SAI-1.5 and SSP2-4.5.

https://doi.org/10.5194/egusphere-2025-3151
Preprint. Discussion started: 30 July 2025

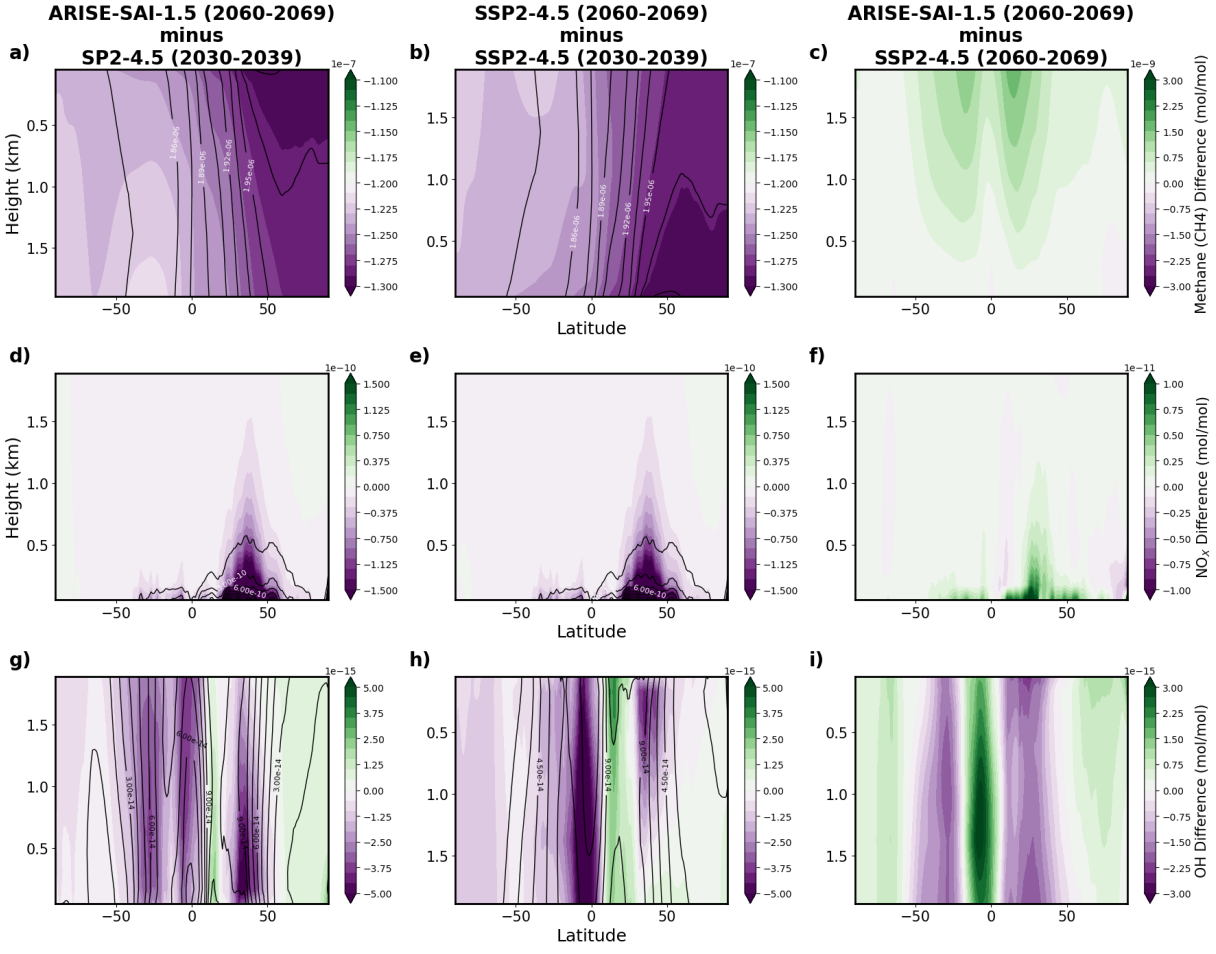

Figure A5. Zonal-mean differences in methane (a-b), NO_X (d-f), and OH (g-i) concentrations (mol mol^{-1}) are presented for ARISE-SAI-1.5 (2060–2069) minus SSP2-4.5 (2030–2039), SSP2-4.5 (2060–2069) minus SSP2-4.5 (2030–2039), and ARISE-SAI-1.5 (2060–2069) minus SSP2-4.5 (2060–2069). Shading indicates the concentration differences, with black contours in the first two columns showing the absolute zonal-mean concentrations.

https://doi.org/10.5194/egusphere-2025-3151
Preprint. Discussion started: 30 July 2025

Author contributions. CW performed the analysis of the model simulations and wrote the manuscript. DV helped outline and write the manuscript and provided insight on the analyses. GC provided guidance on how to conduct the mortality calculations and helped write the manuscript. EB provided insight on the analysis and contributed to the writing of the manuscript.

Competing interests. At least one of the (co-)authors is a member of the editorial board of Atmospheric Chemistry and Physics.

Acknowledgements. CW and DV acknowledge financial support by the Quadrature Climate Foundation. We thank Douglas G. MacMartin for his constructive discussions and suggestions during the development of this work. We would also like to thank Yutang Xiong and Collin Meisel at the Frederick S. Pardee Institute for International Futures for their help with accessing the IFS platform and quick response to inquiries.

https://doi.org/10.5194/egusphere-2025-3151
Preprint. Discussion started: 30 July 2025

References

Archibald, A. T., Turnock, S. T., Griffiths, P. T., Cox, T., Derwent, R. G., Knote, C., and Shin, M.: On the changes in surface ozone over the twenty-first century: sensitivity to changes in surface temperature and chemical mechanisms, Philosophical Transactions of the Royal Society A, 378, 20190 329, 2020.

Bednarz, E. M., Visioni, D., Banerjee, A., Braesicke, P., Kravitz, B., and MacMartin, D. G.: The overlooked role of the stratosphere under a solar constant reduction, Geophysical Research Letters, 49, e2022GL098 773, 2022.

Bednarz, E. M., Butler, A. H., Visioni, D., Zhang, Y., Kravitz, B., and MacMartin, D. G.: Injection strategy–a driver of atmospheric circulation and ozone response to stratospheric aerosol geoengineering, Atmospheric Chemistry and Physics, 23, 13 665–13 684, 2023a.

Bednarz, E. M., Visioni, D., Butler, A. H., Kravitz, B., MacMartin, D. G., and Tilmes, S.: Potential non-linearities in the high latitude circulation and ozone response to stratospheric aerosol injection, Geophysical Research Letters, 50, e2023GL104 726, 2023b.

Brauer, M., Roth, G. A., Aravkin, A. Y., Zheng, P., Abate, K. H., Abate, Y. H., Abbafati, C., Abbasgholizadeh, R., Abbasi, M. A., Abbasian, M., et al.: Global burden and strength of evidence for 88 risk factors in 204 countries and 811 subnational locations, 1990–2021: a systematic analysis for the Global Burden of Disease Study 2021, The Lancet, 403, 2162–2203, 2024.

Burnett, R. and Cohen, A.: Relative risk functions for estimating excess mortality attributable to outdoor PM2. 5 air pollution: Evolution and state-of-the-art, Atmosphere, 11, 589, 2020.

Burnett, R., Chen, H., Szyszkowicz, M., Fann, N., Hubbell, B., Pope III, C. A., Apte, J. S., Brauer, M., Cohen, A., Weichenthal, S., et al.: Global estimates of mortality associated with long-term exposure to outdoor fine particulate matter, Proceedings of the National Academy of Sciences, 115, 9592–9597, 2018.

Burnett, R. T., Pope III, C. A., Ezzati, M., Olives, C., Lim, S. S., Mehta, S., Shin, H. H., Singh, G., Hubbell, B., Brauer, M., et al.: An integrated risk function for estimating the global burden of disease attributable to ambient fine particulate matter exposure, Environmental health perspectives, 122, 397–403, 2014.

Center for International Earth Science Information Network (CIESIN) - Columbia University: Gridded Population of the World, Version 4 (GPWv4): National Identifier Grid, Revision 11, https://doi.org/10.7927/H4TD9VDP, [Data set], 2018.

Cheng, W., MacMartin, D. G., Kravitz, B., Visioni, D., Bednarz, E. M., Xu, Y., Luo, Y., Huang, L., Hu, Y., Staten, P. W., et al.: Changes in Hadley circulation and intertropical convergence zone under strategic stratospheric aerosol geoengineering, npj Climate and Atmospheric Science, 5, 32, 2022.

Davis, N. A., Visioni, D., Garcia, R. R., Kinnison, D. E., Marsh, D. R., Mills, M., Richter, J. H., Tilmes, S., Bardeen, C. G., Gettelman, A., Glanville, A. A., MacMartin, D. G., Smith, A. K., and Vitt, F.: Climate, Variability, and Climate Sensitivity of "Middle Atmosphere" Chemistry Configurations of the Community Earth System Model Version 2, Whole Atmosphere Community Climate Model Version 6 (CESM2(WACCM6)), Journal of Advances in Modeling Earth Systems, 15, e2022MS003 579, https://doi.org/https://doi.org/10.1029/2022MS003579, e2022MS003579 2022MS003579, 2023.

Doherty, R., Wild, O., Shindell, D., Zeng, G., MacKenzie, I., Collins, W., Fiore, A., Stevenson, D., Dentener, F., Schultz, M., et al.: Impacts of climate change on surface ozone and intercontinental ozone pollution: A multi-model study, Journal of Geophysical Research: Atmospheres, 118, 3744–3763, 2013.

Eastham, S. D., Weisenstein, D. K., Keith, D. W., and Barrett, S. R.: Quantifying the impact of sulfate geoengineering on mortality from air quality and UV-B exposure, Atmospheric environment, 187, 424–434, 2018.

https://doi.org/10.5194/egusphere-2025-3151
Preprint. Discussion started: 30 July 2025

Fiore, A. M., Naik, V., and Leibensperger, E. M.: Air quality and climate connections, Journal of the Air & Waste Management Association, 65, 645–685, 2015.

Fricko, O., Havlik, P., Rogelj, J., Klimont, Z., Gusti, M., Johnson, N., Kolp, P., Strubegger, M., Valin, H., Amann, M., Ermolieva, T., Forsell, N., Herrero, M., Heyes, C., Kindermann, G., Krey, V., McCollum, D. L., Obersteiner, M., Pachauri, S., Rao, S., Schmid, E., Schoepp, W., and Riahi, K.: The marker quantification of the Shared Socioeconomic Pathway 2: A middle-of-the-road scenario for the 21st century, Global Environmental Change, 42, 251–267, https://doi.org/https://doi.org/10.1016/j.gloenvcha.2016.06.004, 2017.

Gettelman, A., Mills, M. J., Kinnison, D. E., Garcia, R. R., Smith, A. K., Marsh, D. R., Tilmes, S., Vitt, F., Bardeen, C. G., McInerny, J., Liu, H.-L., Solomon, S. C., Polvani, L. M., Emmons, L. K., Lamarque, J.-F., Richter, J. H., Glanville, A. S., Bacmeister, J. T., Phillips, A. S., Neale, R. B., Simpson, I. R., DuVivier, A. K., Hodzic, A., and Randel, W. J.: The Whole Atmosphere Community Climate Model Version 6 (WACCM6), Journal of Geophysical Research: Atmospheres, 124, 12 380–12 403, https://doi.org/https://doi.org/10.1029/2019JD030943, 2019.

Harding, A., Vecchi, G. A., Yang, W., and Keith, D. W.: Impact of solar geoengineering on temperature-attributable mortality, Proceedings of the National Academy of Sciences, 121, e2401801 121, 2024.

Hughes, B., Peterson, C., Rothman, D., and Solorzano, J.: IFs Health Model Documentation, Pardee Center for International Futures, Denver, 2014.

Jacob, D. J. and Winner, D. A.: Effect of climate change on air quality, Atmospheric environment, 43, 51–63, 2009.

Jerrett, M., Burnett, R. T., Pope III, C. A., Ito, K., Thurston, G., Krewski, D., Shi, Y., Calle, E., and Thun, M.: Long-term ozone exposure and mortality, New England Journal of Medicine, 360, 1085–1095, 2009.

Jones, B. and O'Neill, B.: Global one-eighth degree population base year and projection grids based on the shared socioeconomic pathways, revision 01, Palisades, New York: NASA Socioeconomic Data and Applications Center (SEDAC) https://doi. org/10.7927/m30p-j498, 2020.

Kinnison, D., Brasseur, G. P., Walters, S., Garcia, R., Marsh, D., Sassi, F., Harvey, V., Randall, C., Emmons, L., Lamarque, J.-F., et al.: Sensitivity of chemical tracers to meteorological parameters in the MOZART-3 chemical transport model, Journal of Geophysical Research: Atmospheres, 112, 2007.

Kravitz, B., Robock, A., Tilmes, S., Boucher, O., English, J. M., Irvine, P. J., Jones, A., Lawrence, M. G., MacCracken, M., Muri, H., et al.: The geoengineering model intercomparison project phase 6 (GeoMIP6): Simulation design and preliminary results, Geoscientific Model Development, 8, 3379–3392, 2015.

Kravitz, B., MacMartin, D. G., Mills, M. J., Richter, J. H., Tilmes, S., Lamarque, J.-F., Tribbia, J. J., and Vitt, F.: First simulations of designing stratospheric sulfate aerosol geoengineering to meet multiple simultaneous climate objectives, Journal of Geophysical Research: Atmospheres, 122, 12–616, 2017.

Lee, W., MacMartin, D., Visioni, D., and Kravitz, B.: Expanding the design space of stratospheric aerosol geoengineering to include precipitation-based objectives and explore trade-offs, Earth system dynamics, 11, 1051–1072, 2020.

Liu, X., Ma, P.-L., Wang, H., Tilmes, S., Singh, B., Easter, R. C., Ghan, S. J., and Rasch, P. J.: Description and evaluation of a new four-mode version of the Modal Aerosol Module (MAM4) within version 5.3 of the Community Atmosphere Model, Geoscientific Model Development, 9, 505–522, https://doi.org/10.5194/gmd-9-505-2016, 2016.

Liu, Y., Wang, P., Li, Y., Wen, L., and Deng, X.: Air quality prediction models based on meteorological factors and real-time data of industrial waste gas, Scientific Reports, 12, 9253, 2022.

https://doi.org/10.5194/egusphere-2025-3151
Preprint. Discussion started: 30 July 2025

Malashock, D. A., Delang, M. N., Becker, J. S., Serre, M. L., West, J. J., Chang, K.-L., Cooper, O. R., and Anenberg, S. C.: Global trends in ozone concentration and attributable mortality for urban, peri-urban, and rural areas between 2000 and 2019: a modelling study, The Lancet Planetary Health, 6, e958–e967, 2022.

McCormick, M. P., Thomason, L. W., and Trepte, C. R.: Atmospheric effects of the Mt Pinatubo eruption, Nature, 373, 399–404, 1995.

Moch, J. M., Mickley, L. J., Eastham, S. D., Lundgren, E. W., Shah, V., Buonocore, J. J., Pang, J. Y. S., Sadiq, M., and Tai, A. P. K.: Overlooked Long-Term Atmospheric Chemical Feedbacks Alter the Impact of Solar Geoengineering: Implications for Tropospheric Oxidative Capacity, AGU Advances, 4, e2023AV000 911, https://doi.org/https://doi.org/10.1029/2023AV000911, 2023.

Murray, C. J., Aravkin, A. Y., Zheng, P., Abbafati, C., Abbas, K. M., Abbasi-Kangevari, M., Abd-Allah, F., Abdelalim, A., Abdollahi, M., Abdollahpour, I., et al.: Global burden of 87 risk factors in 204 countries and territories, 1990–2019: a systematic analysis for the Global Burden of Disease Study 2019, The lancet, 396, 1223–1249, 2020.

Niemeier, U. and Schmidt, H.: Changing transport processes in the stratosphere by radiative heating of sulfate aerosols, Atmospheric Chemistry and Physics, 17, 14 871–14 886, 2017.

Niu, Y., Zhou, Y., Chen, R., Yin, P., Meng, X., Wang, W., Liu, C., Ji, J. S., Qiu, Y., Kan, H., et al.: Long-term exposure to ozone and cardiovascular mortality in China: a nationwide cohort study, The Lancet Planetary Health, 6, e496–e503, 2022.

Norman, O. G., Heald, C. L., Bililign, S., Campuzano-Jost, P., Coe, H., Fiddler, M. N., Green, J. R., Jimenez, J. L., Kaiser, K., Liao, J., et al.: Exploring the processes controlling secondary inorganic aerosol: evaluating the global GEOS-Chem simulation using a suite of aircraft campaigns, Atmospheric Chemistry and Physics, 25, 771–795, 2025.

Organization, W. H. et al.: WHO global air quality guidelines: particulate matter (PM2. 5 and PM10), ozone, nitrogen dioxide, sulfur dioxide and carbon monoxide, World Health Organization, 2021.

Peng, L., Liu, F., Zhou, M., Li, M., Zhang, Q., and Mauzerall, D. L.: Alternative-energy-vehicles deployment delivers climate, air quality, and health co-benefits when coupled with decarbonizing power generation in China, One Earth, 4, 1127–1140, 2021.

Rasmussen, D., Hu, J., Mahmud, A., and Kleeman, M. J.: The ozone–climate penalty: past, present, and future, Environmental science & technology, 47, 14 258–14 266, 2013.

Riahi, K., Van Vuuren, D. P., Kriegler, E., Edmonds, J., O'neill, B. C., Fujimori, S., Bauer, N., Calvin, K., Dellink, R., Fricko, O., et al.: The Shared Socioeconomic Pathways and their energy, land use, and greenhouse gas emissions implications: An overview, Global environmental change, 42, 153–168, 2017.

Richter, J. and Visioni, D.: ARISE-SAI-1.5: Assessing Responses and Impacts of Solar climate intervention on the Earth system with Stratospheric Aerosol Injection, with cooling to 1.5C [Data set], https://doi.org/10.5281/zenodo.6473775, 2022a.

Richter, J. and Visioni, D.: SSP2-4.5 Simulations with CESM2 (WACCM6), Zenodo[Data set], https://doi.org/10.5281/zenodo.6473953, 2022b.

Richter, J. H., Visioni, D., MacMartin, D. G., Bailey, D. A., Rosenbloom, N., Dobbins, B., Lee, W. R., Tye, M., and Lamarque, J.-F.: Assessing Responses and Impacts of Solar climate intervention on the Earth system with stratospheric aerosol injection (ARISE-SAI): protocol and initial results from the first simulations, Geoscientific Model Development, 15, 8221–8243, 2022.

Robock, A.: Volcanic eruptions and climate, Reviews of geophysics, 38, 191–219, 2000.

Samir, K. and Lutz, W.: The human core of the shared socioeconomic pathways: Population scenarios by age, sex and level of education for all countries to 2100, Global Environmental Change, 42, 181–192, 2017.

https://doi.org/10.5194/egusphere-2025-3151
Preprint. Discussion started: 30 July 2025

Sun, H. Z., van Daalen, K. R., Morawska, L., Guillas, S., Giorio, C., Di, Q., Kan, H., Loo, E. X.-L., Shek, L. P., Watts, N., et al.: An estimate of global cardiovascular mortality burden attributable to ambient ozone exposure reveals urban-rural environmental injustice, One Earth, 7, 1803–1819, 2024.

Tilmes, S., Garcia, R. R., Kinnison, D. E., Gettelman, A., and Rasch, P. J.: Impact of geoengineered aerosols on the troposphere and stratosphere, Journal of Geophysical Research: Atmospheres, 114, 2009.

Tilmes, S., Richter, J. H., Kravitz, B., MacMartin, D. G., Mills, M. J., Simpson, I. R., Glanville, A. S., Fasullo, J. T., Phillips, A. S., Lamarque, J.-F., et al.: CESM1 (WACCM) stratospheric aerosol geoengineering large ensemble project, Bulletin of the American Meteorological Society, 99, 2361–2371, 2018.

Tilmes, Simone, V.-D., Jones, A., Haywood, J., Séférian, R., Nabat, P., Boucher, O., Bednarz, E. M., Niemeier, U., et al.: Stratospheric ozone response to sulfate aerosol and solar dimming climate interventions based on the G6 Geoengineering Model Intercomparison Project (GeoMIP) simulations, Atmospheric Chemistry and Physics, 22, 4557–4579, 2022.

Tracy, S. M., Moch, J. M., Eastham, S. D., and Buonocore, J. J.: Stratospheric aerosol injection may impact global systems and human health outcomes, Elem Sci Anth, 10, 00 047, 2022.

Turnock, S. T., Allen, R. J., Andrews, M., Bauer, S. E., Deushi, M., Emmons, L., Good, P., Horowitz, L., John, J. G., Michou, M., et al.: Historical and future changes in air pollutants from CMIP6 models, Atmospheric Chemistry and Physics, 20, 14 547–14 579, 2020.

Vandyck, T., Keramidas, K., Kitous, A., Spadaro, J. V., Van Dingenen, R., Holland, M., and Saveyn, B.: Air quality co-benefits for human health and agriculture counterbalance costs to meet Paris Agreement pledges, Nature Communications, 9, 4939, https://doi.org/10.1038/s41467-018-06885-9, 2018.

Visioni, D., Slessarev, E., MacMartin, D. G., Mahowald, N. M., Goodale, C. L., and Xia, L.: What goes up must come down: impacts of deposition in a sulfate geoengineering scenario, Environmental Research Letters, 15, https://doi.org/https://iopscience.iop.org/article/10.1088/1748-9326/ab94eb, 2020.

Visioni, D., MacMartin, D. G., and Kravitz, B.: Is turning down the sun a good proxy for stratospheric sulfate geoengineering?, Journal of Geophysical Research: Atmospheres, 126, e2020JD033 952, 2021.

Visioni, D., Tilmes, S., Bardeen, C., Mills, M., MacMartin, D. G., Kravitz, B., and Richter, J. H.: Limitations of assuming internal mixing between different aerosol species: a case study with sulfate geoengineering simulations, Atmospheric Chemistry and Physics, 22, 1739–1756, https://doi.org/10.5194/acp-22-1739-2022, 2022.

Visioni, D., Bednarz, E. M., MacMartin, D. G., Kravitz, B., and Goddard, P. B.: The Choice of Baseline Period Influences the Assessments of the Outcomes of Stratospheric Aerosol Injection, Earth's Future, 11, e2023EF003 851, https://doi.org/https://doi.org/10.1029/2023EF003851, e2023EF003851 2023EF003851, 2023.

Wang, C.: Postprocessing code to calculate mortality rates for this paper, Zenodo[code], https://doi.org/10.5281/zenodo.15696232, 2025.

Xia, L., Nowack, P. J., Tilmes, S., and Robock, A.: Impacts of stratospheric sulfate geoengineering on tropospheric ozone, Atmospheric Chemistry and Physics, 17, 11 913–11 928, 2017.

Xu, Z., Chen, S. X., and Wu, X.: Meteorological change and impacts on air pollution: Results from North China, Journal of Geophysical Research: Atmospheres, 125, e2020JD032 423, 2020.

Zanis, P., Akritidis, D., Turnock, S., Naik, V., Szopa, S., Georgoulias, A. K., Bauer, S. E., Deushi, M., Horowitz, L. W., Keeble, J., et al.: Climate change penalty and benefit on surface ozone: a global perspective based on CMIP6 earth system models, Environmental Research Letters, 17, 024 014, 2022.